CFD Final Project: Axial Flow Compressor

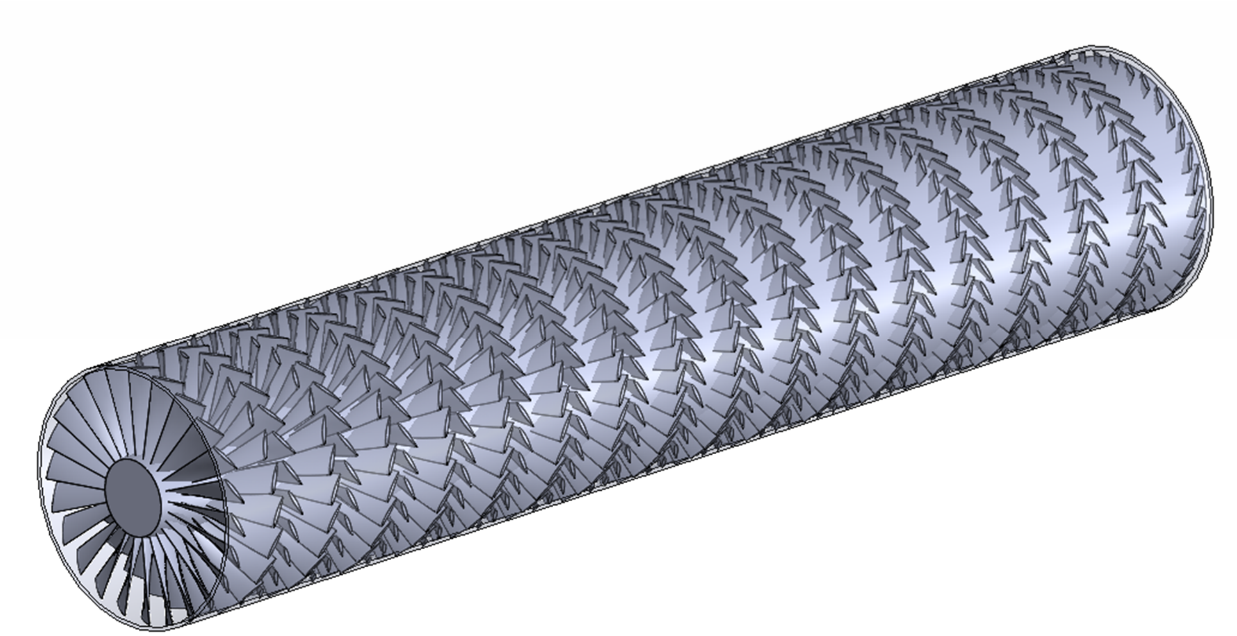

Matthew Bartolomeo, Michael Colella,
Pranav Joneja, Jacob Maarek

ME 407 Professor Bondi
Computational Fluid Dynamics Spring 2018

Table of Contents

Introduction

This paper outlines the design and analysis of an axial flow compressor for a gas turbofan engine. The compressor is to be used to increase the density of intake air prior to combustion. The compressor is to provide a minimum pressure ratio of 20:1 at a prescribed altitude of 37,000 feet. The outer diameter of the blades shall be between 4 feet and 6 feet, and the operating speed shall be below 65,000 RPM for all stages of the compressor. The simulations are to be conducted on a test stand with the fluid condition prescribed at 37,000 feet. The overall design parameters and metrics are outlined in the table below:

Table 1: Dimensions and Design Parameters

Final Compressor Design	
Outer Diameter	66 inches
Inner Diameter	20 – 62.64 inches
Stage Length	20 inches
Number of Blades Per Stage	24 – 36
Number of Stages	17
Operating Speed	6,000 RPM
Rotor/Stator Chord Length	8 inches
Blade Solidity	1.4
Rotor/Stator Airfoil Type	NACA 6512
Rotor/Stator Angle of Twist	1.5 deg/inch
Compression Ratio Per Stage	1.18 – 1.21
Overall Compression Ratio	20.04:1
Power Usage	278,904 hp

The design goal of this project is to produce the required compression ratio while optimizing efficiency of the compressor and minimizing the power requires to operate the compressor.

Design Concept and Assumptions

The design concept for this compressor focuses on optimizing the rotor and stator geometry to maximize efficiency and compression ratio. Performing a literature review of compressor designs produced by NASA and The Boyce Consultancy Group, LLC, we chose the operating parameters for this compressor [1, 2].

The design focuses on optimizing the rotor blade angle of the compressor blades. According to the operating RPM of the compressor and the radius of the blades, the relative air velocity over the airfoil blade is determined. The design resulted in an optimal blade angle at the respective radius. Next, a NACA airfoil was chosen that would not stall at the designed optimal blade angle. The geometry for each stage was then finalized and tested using ANSYS Fluent for varying sizes and RPMs to construct the entire compressor.

The material properties for air were determined from the altitude specification in the problem statement using a NASA study on the properties of air at different heights [3]. These results are replicated in the table below:

Table 2: Air Properties

Parameter	**Value at STP**	**Value at 37,000'**
Pressure	14.7 psi	3.142 psi
Temperature	518.7 R	390 R
Density (initially)	0.0765 lb/ft^3	0.0217 lb/ft^3
Viscosity	$1.202*10^{-5}$ lb/ft-s	$9.55*10^{-6}$ lb/ft-s
Thermal Conductivity	0.0141 BTU/hr-ft-R	0.0113 BTU/hr-ft-R
Specific Heat Capacity	0.24 BTU/lb-R	

The assumptions to be made are the following:

- The engine is to be tested under test stand conditions.
- The engine inlet conditions are to be subsonic.
- The air entering the engine is at the standard conditions for the specified altitude.
- The exhaust tube must match the exact diameter of the final stage of the compressor.

The design dimensions of the compressor are determined largely using hand calculations and are validated using multiple CFD simulations of select compressor stages. We chose to model the first, eighth, and last stage of the compressor to ensure that the calculated compression ratio for each stage is appropriate throughout the compressor.

Compressor Design Theory: Hand Calculations

We begin this section with a discussion on how the rotor hub profile is determined. Because a relatively tight restriction is placed on the outer diameter of the compressor, we opted to adjust the inner diameter for each stage while keeping the outer diameter constant. The inner diameter is determined via mass conservation:

$$\rho_1 A_1 V_1 = \rho_2 A_2 V_2$$

Per axial flow compressor theory, the velocity in the axial direction is constant; the ratio of areas is equal to the ratio of densities per mass conservation. Assuming that air is an ideal gas, the inner diameter at position 2 can be expressed in terms of the inner diameter, pressure, and temperature at position 1, the pressure and temperature at position 2, and the outer diameter:

$$D_{i,2} = \sqrt{D_o^2 - (D_o^2 - D_{i,1}^2)(\frac{P_1}{P_2})(\frac{T_2}{T_1})}$$

The pressure ratio is the same for each stage (1.2). The temperature ratio is determined using the isentropic relationship for an ideal gas:

$$\frac{T_2}{T_1} = (\frac{P_2}{P_1})^{\frac{k-1}{k}}$$

Choosing an initial outer and inner diameter (66 inches and 20 inches, respectively) allows for the remaining inner diameters to be calculated in turn. This procedure also makes it easy to visualize the temperature, pressure, and diameter for each stage.

We determined the number of blades to use for each stage by using a constant blade solidity of 1.4; this value is well within the range of acceptable blade solidities for a modern subsonic compressor [2]. Because the rotor and stator chord length and blade solidity are both constant, the spacing between blades is now also constant. This blade spacing is related to the number of blades by:

$$N = \frac{\pi(\frac{D_o + D_i}{2})}{s}$$

The NACA 6512 airfoil was chosen for both the rotor and stator based on the recommendations for a modern subsonic compressor [1]. At high Reynolds numbers, the stall of this airfoil is gradual, unlike the sharp drop off characteristic of smaller camber airfoils. This was desirable, as it would decrease sensitivity of the airfoils to flow conditions. Because NACA 6512 has a stall angle of about 15 degrees, we put design focus into ensuring no portion of the blade would stall at any distance away from the hub. Because the velocity of the rotor tips is greater than that of the rotor roots, the blade angle of attack will have to change continuously along the length of the blade to keep the blade from stalling.

Figure 1: NACA 6512 geometry [4]

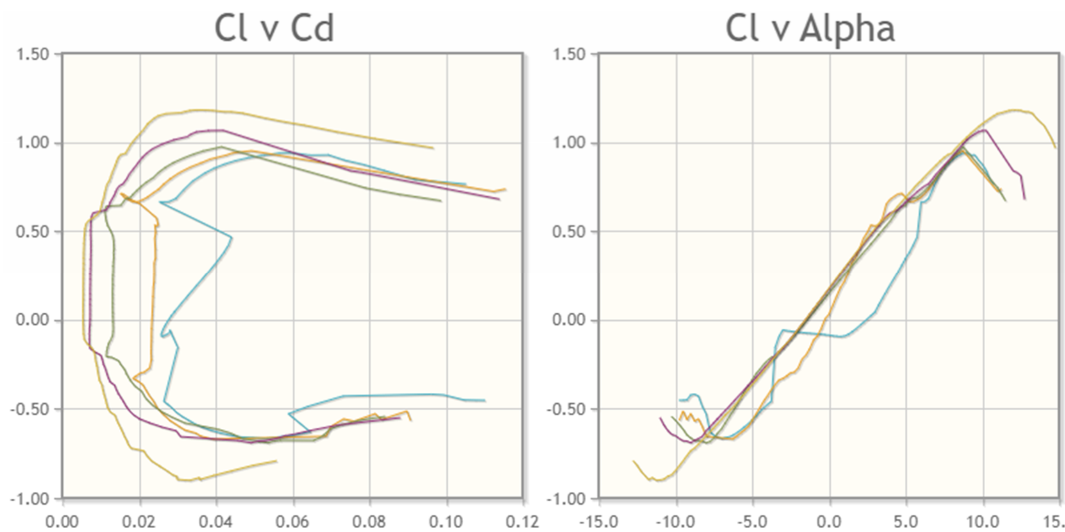

Figure 2: NACA 6512 lift, drag, and angle of attack graphs [4]

The governing equations used to derive the power consumption for the compressor are obtained from basic axial flow compressor theory. Many of these equations can be derived from a velocity triangle diagram, as is shown below.

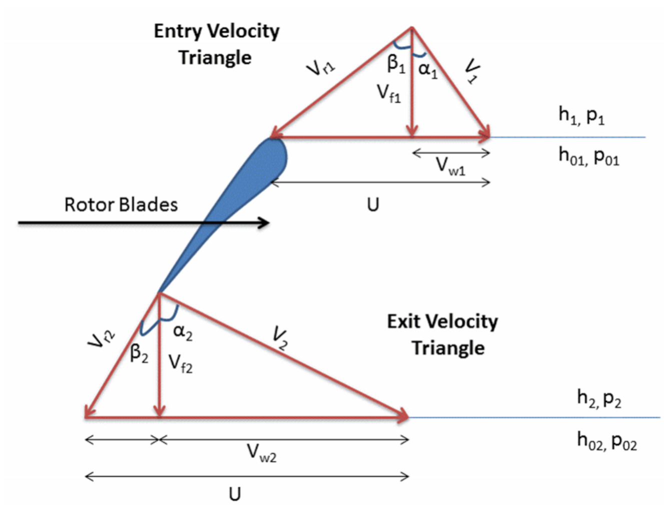

Figure 3: Velocity triangle diagram for rotor [5]

Note here that β_1 and β_2 are geometrically related to the angles of attack for the leading and trailing edges of the blade, respectively. U represents the average linear velocity of the blade at its midline. V_{f1} and V_{f2} represent the velocity in the axial direction before and after the blade, respectively. From the theory of axial flow compressors, it is known that $V_{f1} = V_{f2} = V_f$ (velocity in the axial direction is constant).

The rotation speed for each rotor is chosen to be 6,000 RPM based on the typical operating conditions of modern subsonic axial flow compressors [2]. The median translational rotor velocity due to rotation is given by:

$$U = \frac{\pi \frac{D_o + D_i}{2} RPM}{60}$$

Based on typical axial velocities for other subsonic axial flow compressors and axial velocities that did not cause reversed flow in simulation, a constant axial velocity of 697 fps was used in all calculations.

Blade angle β_1 can be calculated as:

$$\beta_1 = \tan^{-1}(\frac{U}{V_f})$$

Blade angle β_2 is equivalent to the angle of the blade relative to the axial direction.

The power for each stage can be calculated as:

$$P = \dot{m} U V_f (\tan(\beta_1) - \tan(\beta_2))$$

We can calculate the isentropic efficiency of each stage as:

$$\eta_{s,stage} = \frac{\Delta h_{ideal}}{\Delta h_{actual}},$$

where

$$\Delta h_{ideal} = c_p (T_{2s} - T_1)$$

$$\Delta h_{actual} = U V_f (\tan(\beta_1) - \tan(\beta_2))$$

Putting everything together, all formulas and initial conditions are input into an Excel spreadsheet and are optimized to obtain the highest realistic pressure ratio consistently across each stage until a final pressure ratio of 20:1 is obtained. The constant pressure ratio is assumed to be 1.2, as literature has proven that efficiency can realistically be maximized when the flow is subsonic.

The hand calculation results for each stage for 37,000’ and STP air conditions are summarized below:

Table 3: 37,000’ Hand Calculation Results

Stage	Inlet Density (lb/ft^3)	Temperature (R)	Pressure (psi)	Inner Diameter (in)	Power (hp)	Efficiency (%)
1	0.0217	390	3.14	20	10,558	78
2	0.0248	411	3.77	29.72	12,971	75
3	0.0282	433	4.52	36.15	14,165	75
4	0.0321	456	5.43	40.98	15,329	74
5	0.0366	480	6.51	44.79	15,973	74
6	0.0417	506	7.82	47.89	16,505	75
7	0.0475	533	9.38	50.45	16,962	75
8	0.0541	562	11.26	52.59	17,401	76
9	0.0616	592	13.51	54.41	17,728	76
10	0.0702	623	16.21	55.95	17,809	77
11	0.0800	657	19.45	57.27	18,223	78
12	0.0911	692	23.34	58.41	18,045	79
13	0.1038	729	28.01	59.39	18,237	80
14	0.1182	768	33.62	60.23	18,297	81
15	0.1346	809	40.34	60.97	18,393	82
16	0.1534	852	48.41	61.60	18,458	84
17	0.1747	897	58.09	62.16	18,518	85
Total Power Consumed: 283,573 hp						

Table 4: STP Hand Calculation Results

Stage	Inlet Density (lb/ft^3)	Temperature (R)	Pressure (psi)	Inner Diameter (in)	Power (hp)	Efficiency (%)
1	0.0765	519	14.70	20	36,924	86
2	0.0871	546	17.64	29.72	45,338	82
3	0.0992	576	21.16	36.15	49,372	81
4	0.1130	606	25.39	40.98	53,380	81
5	0.1288	639	30.47	44.79	55,508	81
6	0.1467	673	36.57	47.89	57,262	82
7	0.1671	709	43.88	50.45	58,770	82
8	0.1903	747	52.66	52.59	60,240	83
9	0.2168	787	63.19	54.41	61,317	84
10	0.2469	829	75.83	55.95	61,498	85
11	0.2813	873	90.99	57.27	62,934	86
12	0.3204	920	109.19	58.41	62,177	88
13	0.3649	969	131.03	59.39	62,813	89
14	0.4157	1,021	157.24	60.23	62,967	91
15	0.4735	1,076	188.68	60.97	63,263	92
16	0.5394	1,133	266.42	61.60	63,452	94
17	0.6144	1,194	271.70	62.16	63,629	96
Total Power Consumed: 980,845 hp						

Compressor Design: First Stage Model

Motivation:
As is discussed in the *Design Concept and Assumptions*, the primary purpose of this model is help verify the governing hand calculations used to characterize the compressor. Using the same initial conditions as are in these calculations, pressure, temperature, and velocity is better characterized in the compressor, and the hand calculations are effectively validated.

Geometry and Mesh:
The geometry of the first stage consists of a set of rotor blades, a set of stator blades, and inlet and outlet ducts. We chose to use a set of three blades for each half of the stage (one full blade in the middle and half of a blade on either end of the model) to allow for rotationally periodic conditions to be easily applied. As both the rotor and stator in this stage consists of 24 blades, a 30° model is created to cut the overall cell count down. For these studies, the blades are modeled implicitly (assuming the blades do not directly transfer heat to the air or vice versa). A polyhedral mesh is used to ensure good quality cells around the blades. A summary of meshing parameters and the resulting geometry is shown below:

Table 5: First Stage Model Meshing Parameters

Meshing Parameter	Value
Blade local sizing	0.25 in.
Air local sizing	0.5 in.
Number of blade boundary layers	5
Volume mesh size	0.5 in.
Volume mesh growth rate	1.2
Total number of cells	1,485,273

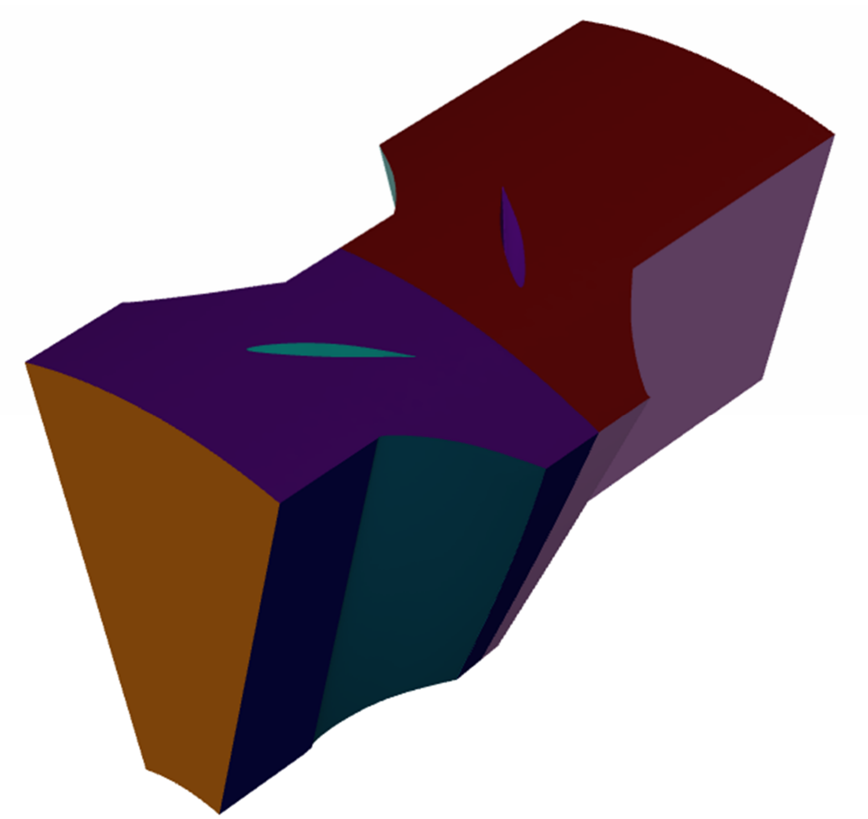

Figure 4: Geometry of the first stage model

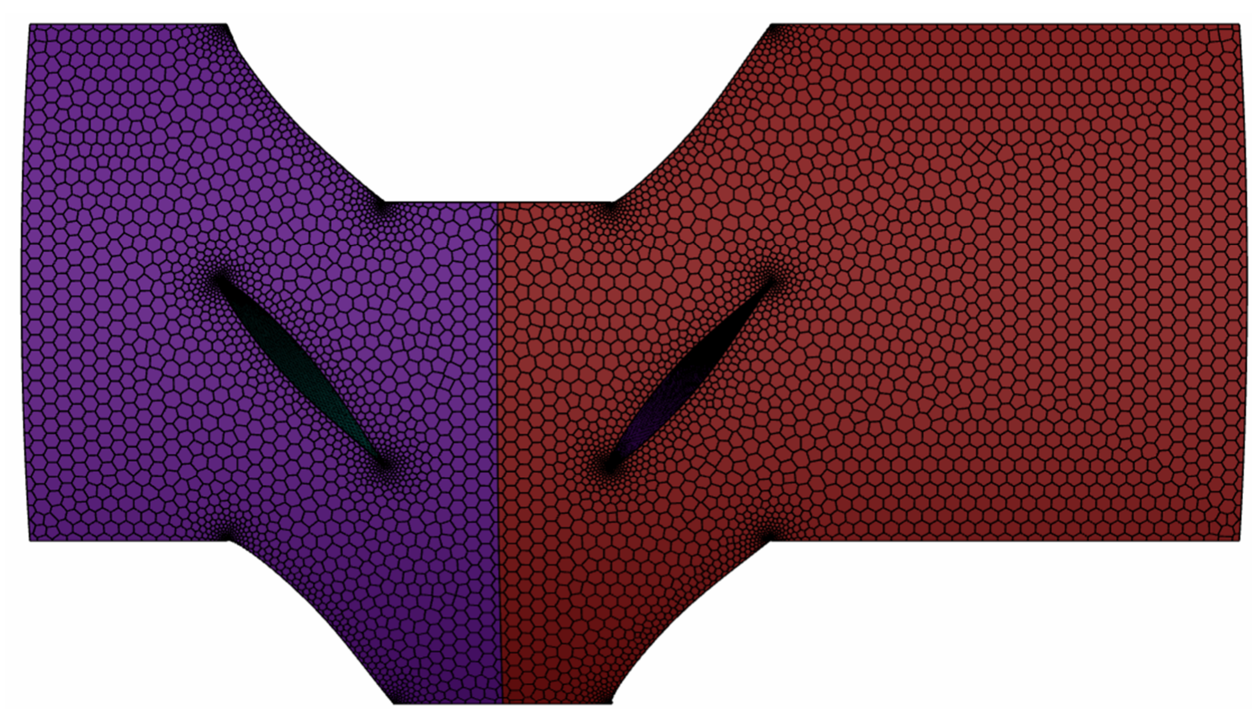

Figure 5: Mesh of the blades and air

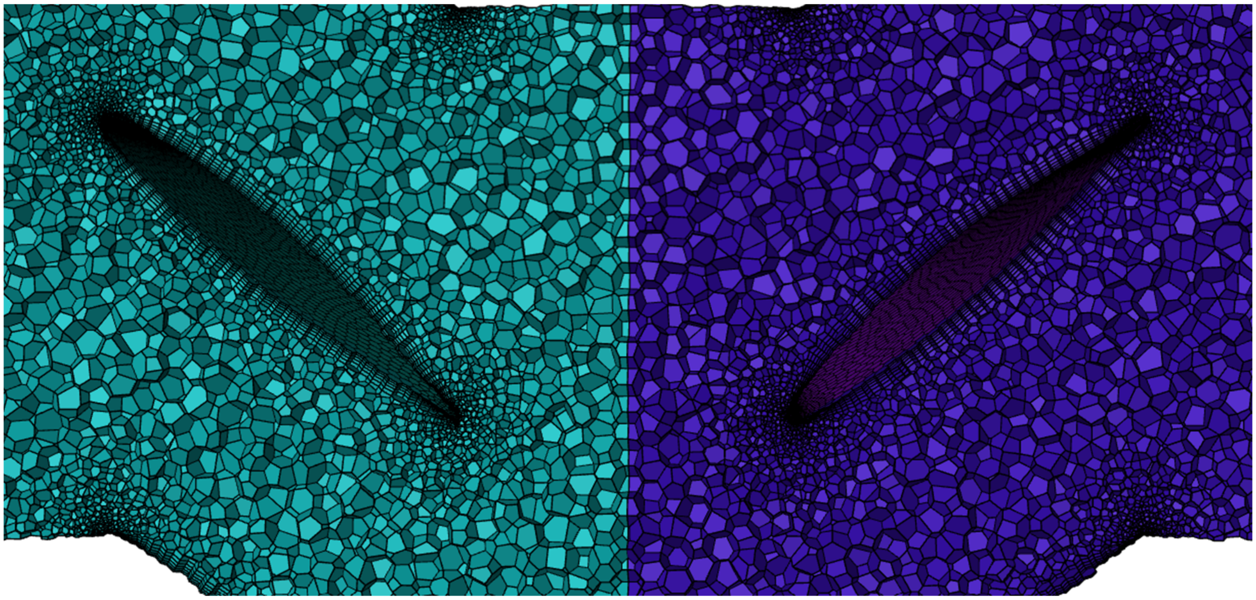

Figure 6: Boundary layers surrounding each blade

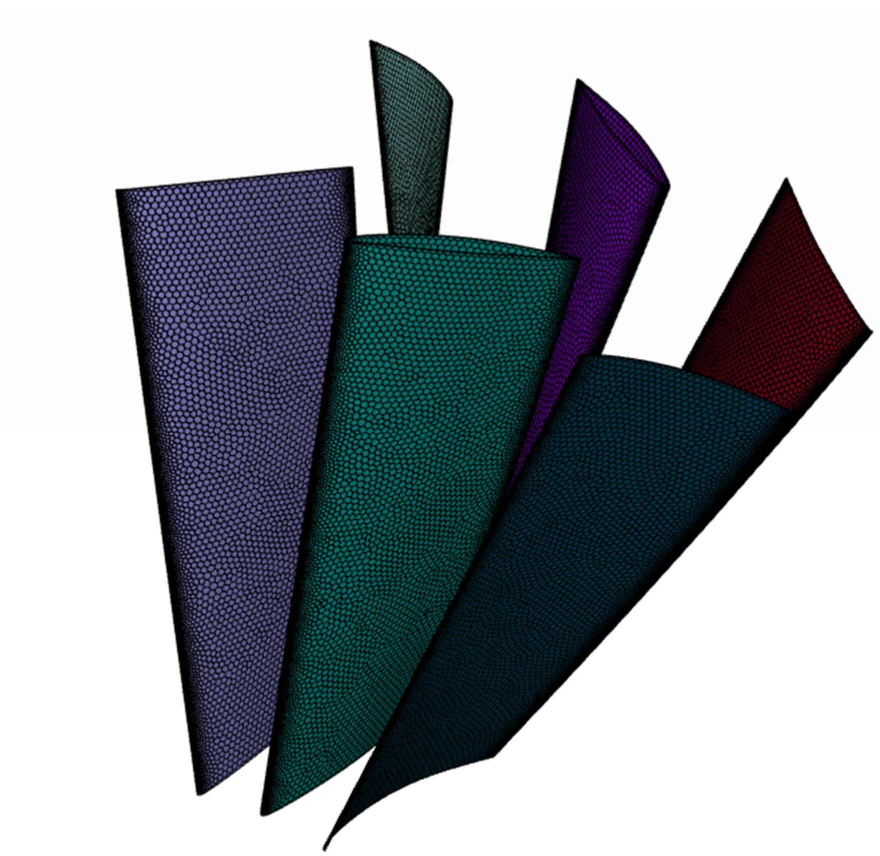

Figure 7: Mesh of blade surface

Material Properties:
The properties for air are calculated for air at 37,000'. The necessary initial conditions are discussed in the *Hand Calculations* section of the report. Given that problem inherently models compressible flow, the ideal gas law is used for the density of air.

Boundary Condition and Solver Settings:
The model is defined as a pressure-based transient model. The energy equation is turned on to allow for changes in temperature, and a realizable k-epsilon with scalable wall treatment turbulence model is applied. For this simulation, the operating conditions set pressure to the outlet pressure of the stage (3.77 psi). The inlet duct is set as a pressure inlet and the outlet duct is set as a pressure outlet.

Rotational periodic boundary conditions are applied to the sides of the model to simulate the entire stage. A mesh interface with periodic repeats is used between the rotor and stator. All other boundaries are treated as non-slip walls. The stator cell zone does not move in the absolute reference frame. The rotor cell zone was given a rotational speed of 6,000 RPM. All simulations are allowed to run for 720 time steps with 10 iterations per time step with a time step size of $4.167*10^{-5}$ s using the Coupled solver with standard initialization based on the inlet. Convergence is monitored through monitors for mass flow rate, absolute pressure, and axial velocity at the inlet, outlet, and interface. A summary of the boundary conditions and solver settings is provided in the table below:

Table 6: First Stage Model Boundary Conditions and Solver Settings

Parameter	Value
Inlet gauge total pressure	0.1282 psi
Inlet initial gauge pressure	-0.6284 psi
Inlet turbulent intensity	3.18%
Inlet turbulent length scale	0.0224 ft
Inlet total temperature	417 R
Outlet gauge pressure	0 psi
Reference pressure	3.77 psi
Outlet turbulent intensity	3.22%
Outlet turbulent length scale	0.0176 ft
Outlet total temperature	438 R
Rotor rotational speed	6,000 RPM
Pressure-velocity coupling scheme	Coupled
Gradient discretization method	Least Squares Cell Based
Pressure discretization method	Second Order
Momentum discretization method	Second Order Upwind
Turbulent kinetic energy discretization method	Second Order Upwind
Turbulent dissipation rate discretization method	Second Order Upwind
Energy discretization method	Second Order Upwind
Transient formulation	Second Order Implicit

Results:
After 720 time steps, all cases reach convergence. Residuals follow a regular sawtooth pattern dropping at least two orders of magnitude each time step, and the mass flow rate, absolute pressure, and axial velocity are stable.

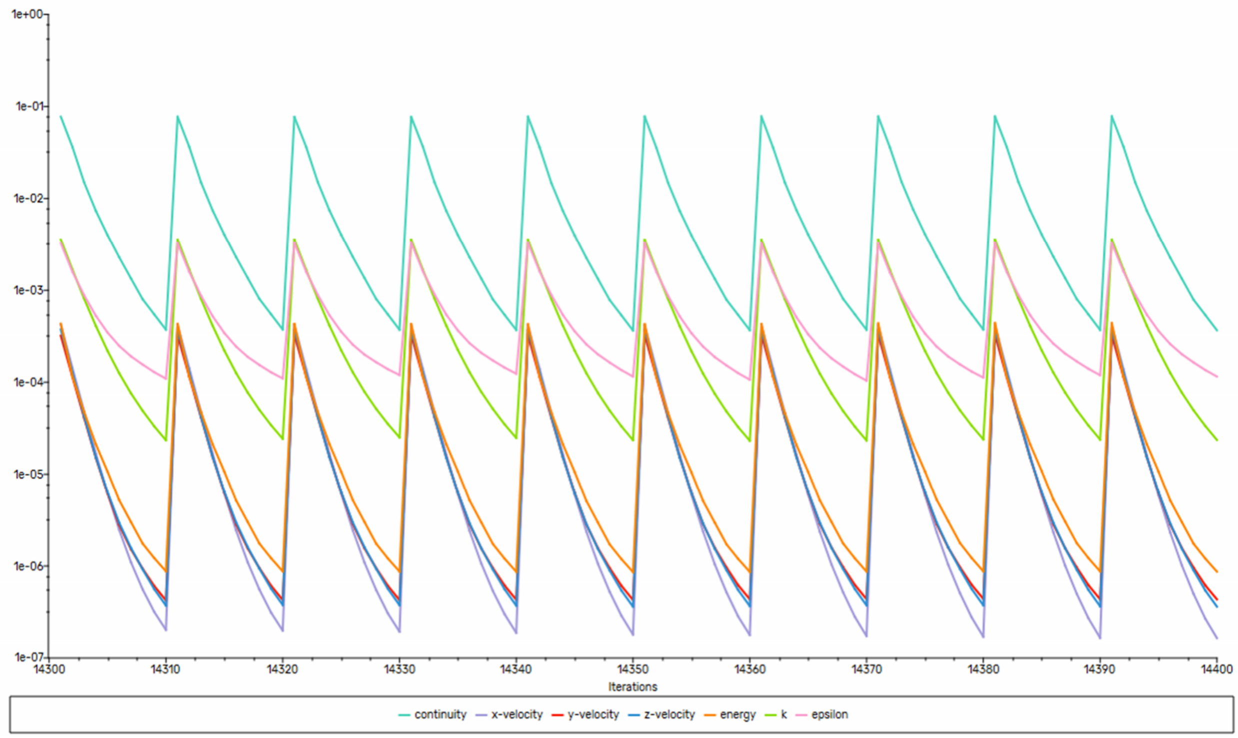

Figure 8: Plots of residuals

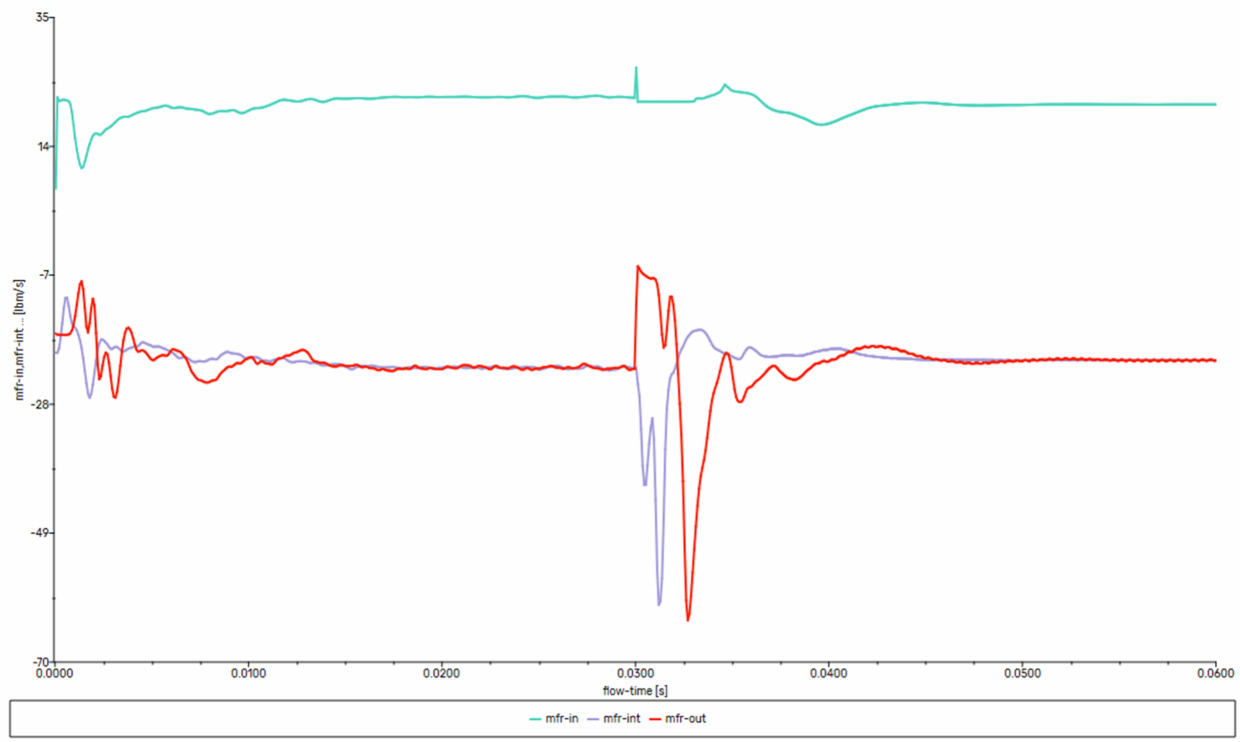

Figure 9: Convergence history for mass flow rate

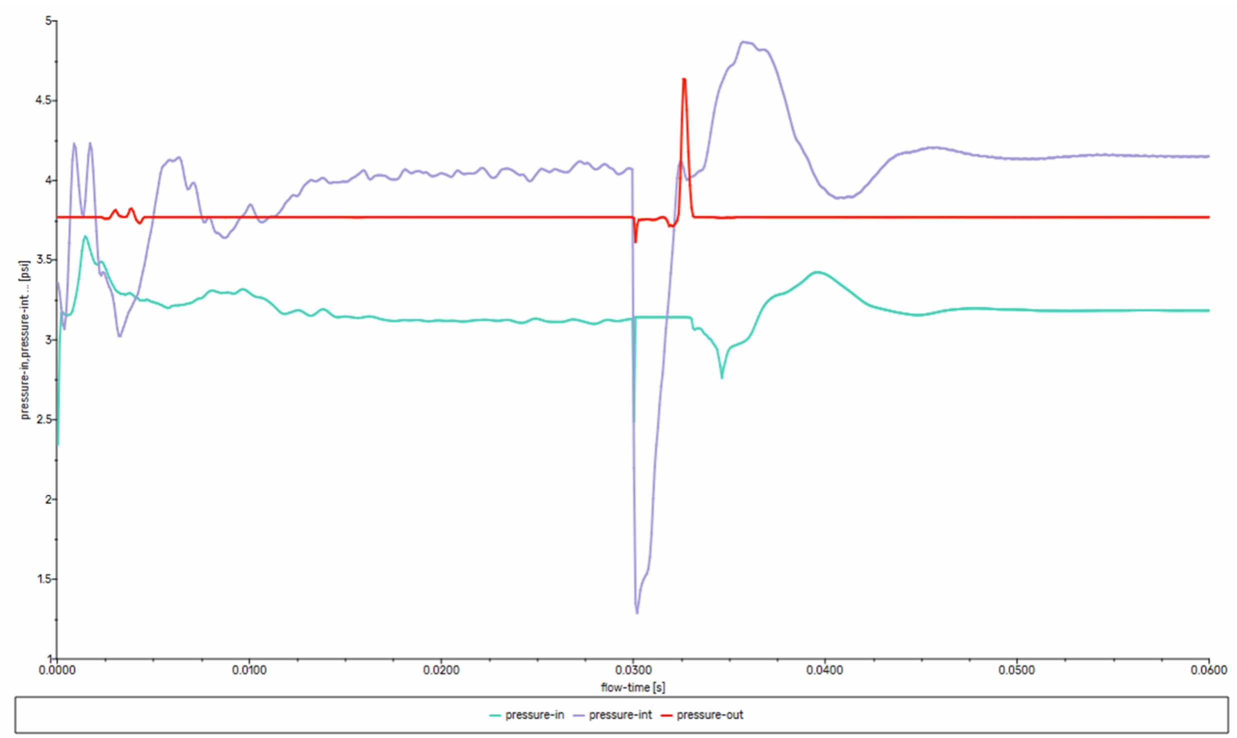

Figure 10: Convergence history for absolute pressure

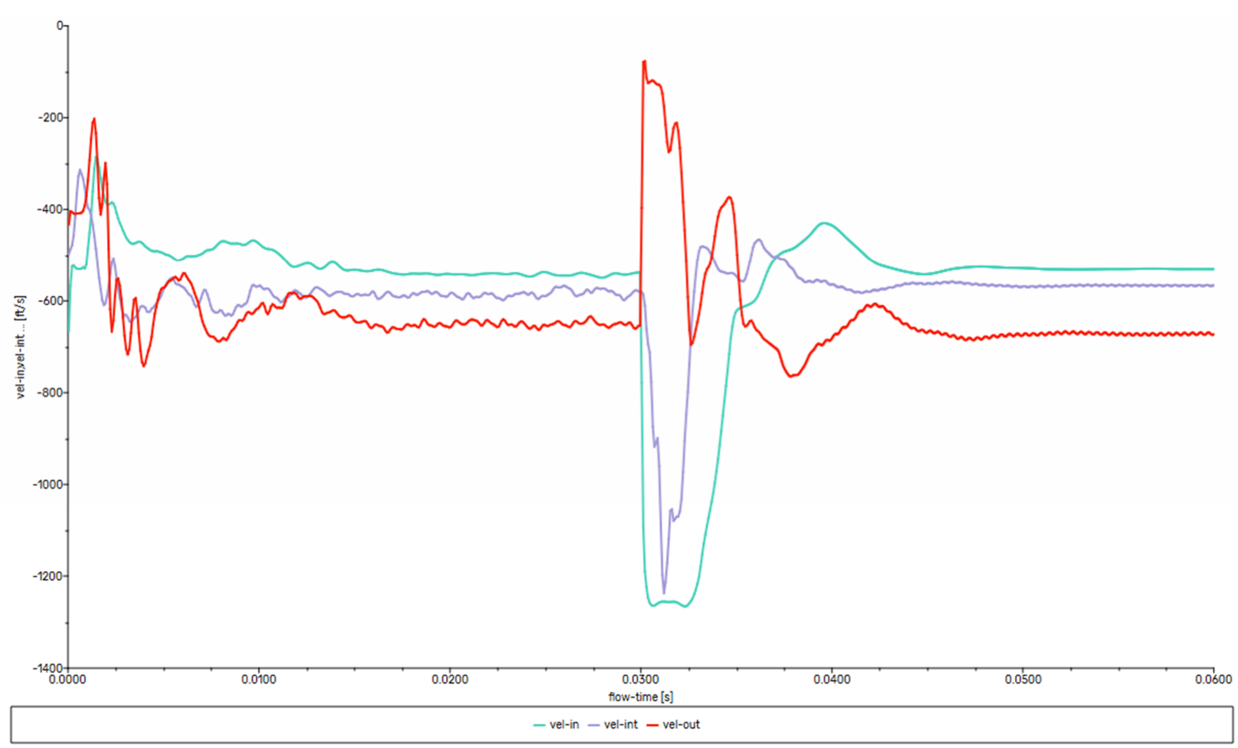

Figure 11: Convergence history of axial velocity

To visualize the behavior inside the compressor, contour plots of pressure and temperature and streamlines of velocity are shown below.

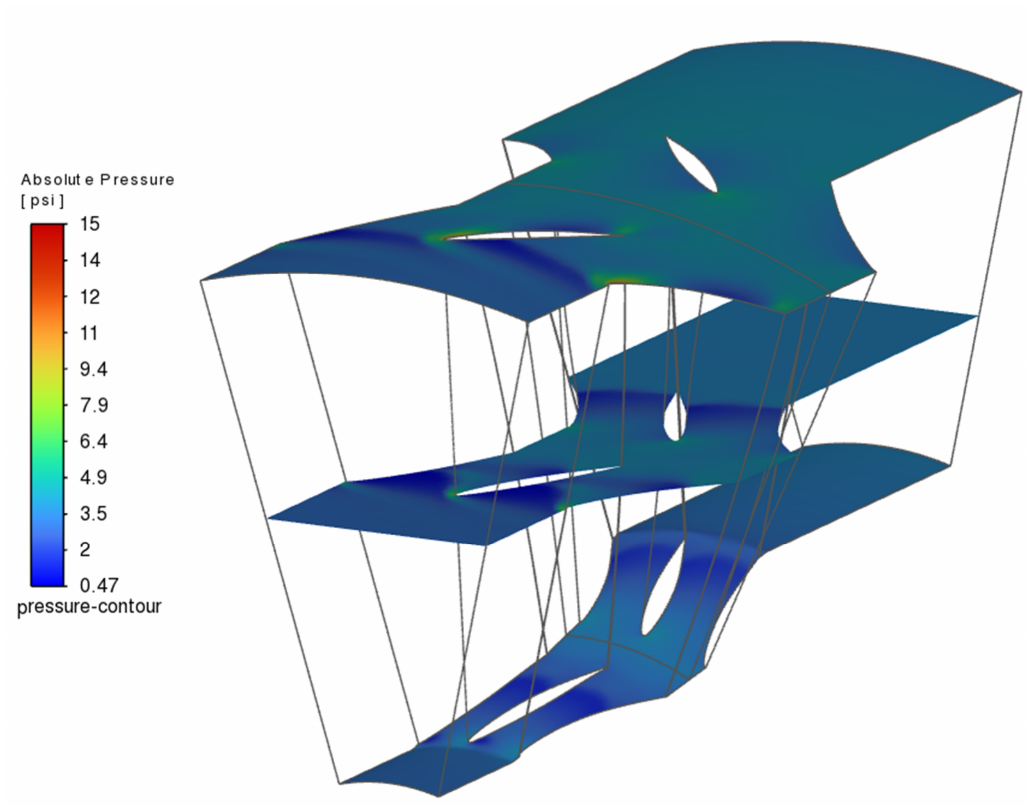

Figure 12: Pressure contour inside the first stage

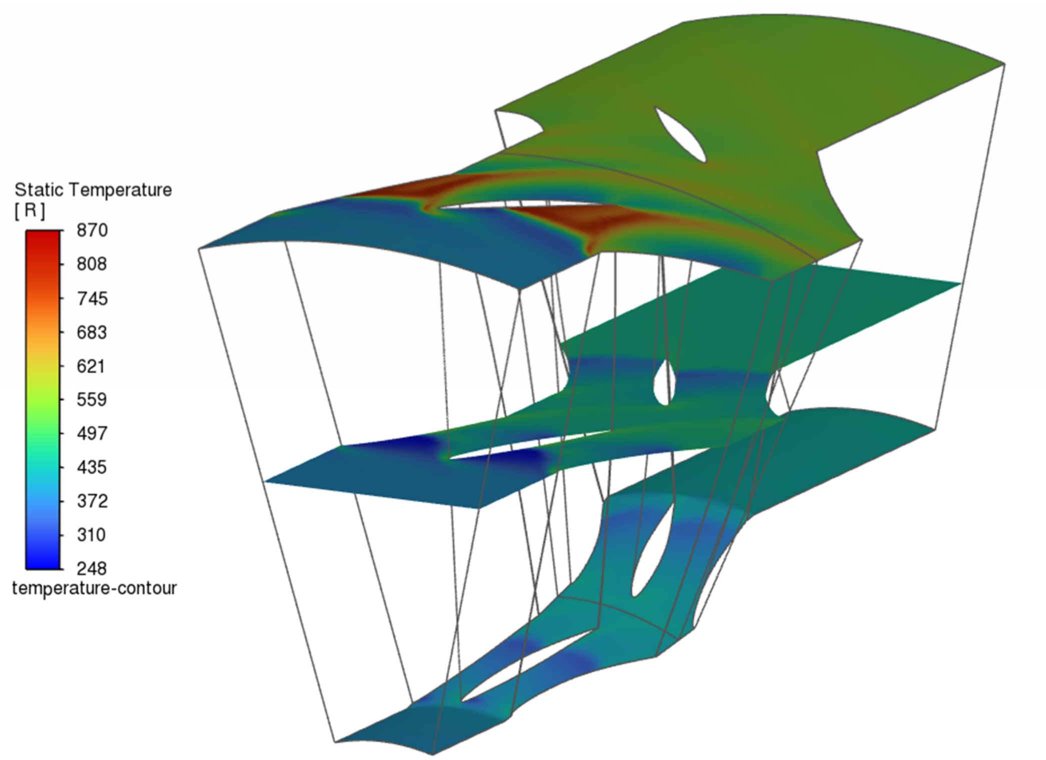

Figure 13: Temperature contour inside the first stage

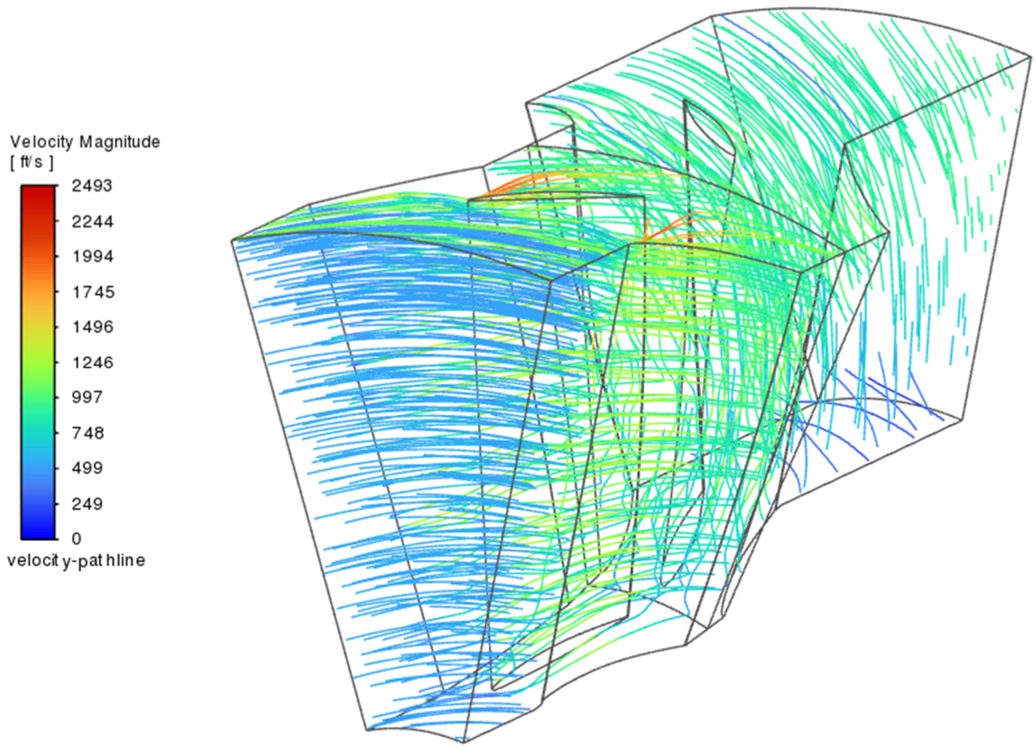

Figure 14: Velocity streamlines around the rotor and stator blades for the first stage

Table 7: Summary of the results for the first stage

Parameter	Value
Mass flow rate	20.86 lb/s
Inlet pressure	3.18 psi
Outlet pressure	3.77 psi
Inlet temperature	393 R
Outlet temperature	481 R
Specific enthalpy change	22.33 BTU/lb
Pressure ratio	1.18

Hand Calculations for Validation:
These results are mostly validated by comparison to the theoretical values computed in the hand calculations above. To calculate the overall mass flow rate, we simply multiply the mass flow

rate of the segment by the number of 30° segments in a 360° compressor (12). To calculate the actual exit temperature, we use the following formula:

$$T_{2,actual} = T_1 + \frac{w_{actual}}{c_p}$$

A summary of the simulation values compared to the hand calculation values is provided in the table below:

Table 8: Comparison of first stage results to hand calculations

Parameter	Simulation Value	Hand Calculation Value
Total mass flow rate	20.78*12 segments = 249.36 lb/s	250.08 lb/s
Inlet pressure	3.18 psi	3.14 psi
Outlet pressure	3.77 psi	3.77 psi
Inlet temperature	393 R	390 R
Outlet temperature	481 R	488 R
Specific enthalpy change	22.33 BTU/lb	23.50 BTU/lb
Pressure ratio	1.18	1.2

Compressor Design: Eighth Stage Model

Motivation:

As is discussed in the *Design Concept and Assumptions*, the primary purpose of this model is help verify the governing hand calculations used to characterize the compressor. Using the same initial conditions as are in these calculations, pressure, temperature, and velocity is better characterized in the compressor, and the hand calculations are effectively validated.

Geometry and Mesh:

The geometry of the eighth stage consists of a set of rotor blades, a set of stator blades, and inlet and outlet ducts. We chose to use a set of three blades for each half of the stage (one full blade in the middle and half of a blade on either end of the model) to allow for rotationally periodic conditions to be easily applied. As both the rotor and stator in this stage consists of 34 blades, a 21.18° model is created to cut the overall cell count down. For these studies, the blades are modeled implicitly (assuming the blades do not directly transfer heat to the air or vice versa). A polyhedral mesh is used to ensure good quality cells around the blades. A summary of meshing parameters and the resulting geometry is shown below:

Table 9: Eighth Stage Model Meshing Parameters

Meshing Parameter	Value
Blade local sizing	0.25 in.
Air local sizing	0.5 in.
Number of blade boundary layers	5
Volume mesh size	0.5 in.
Volume mesh growth rate	1.2
Total number of cells	889,493

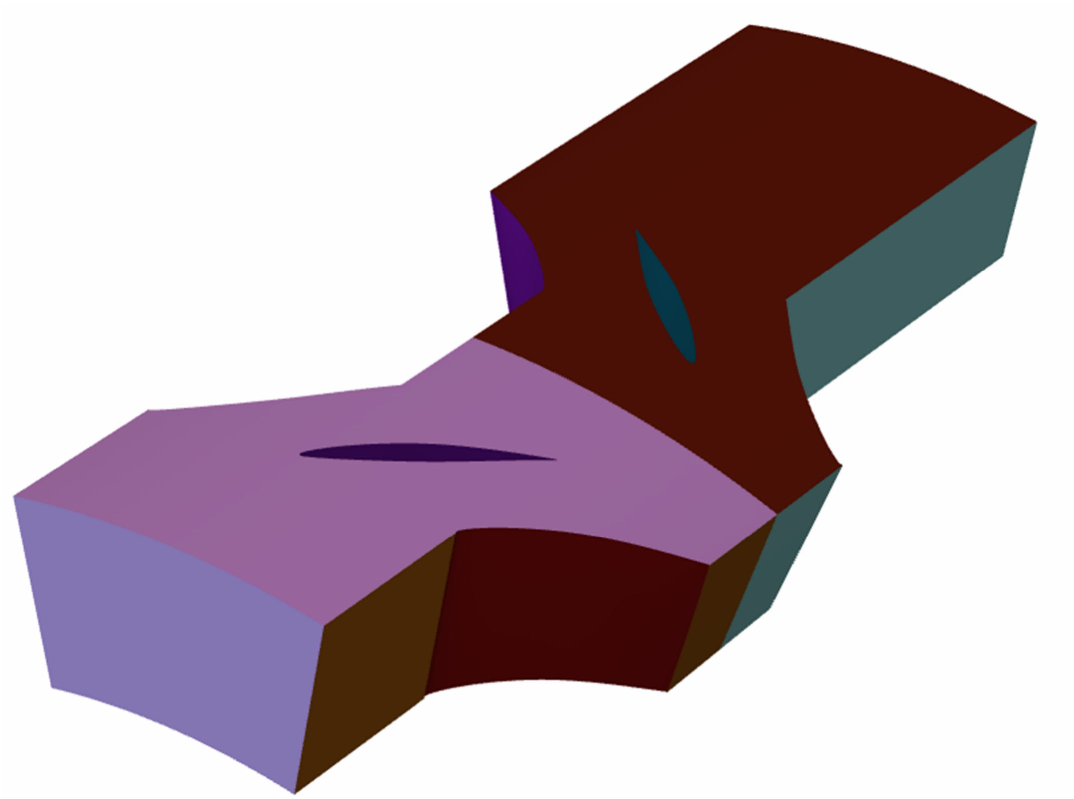

Figure 15: Geometry of the eighth stage model

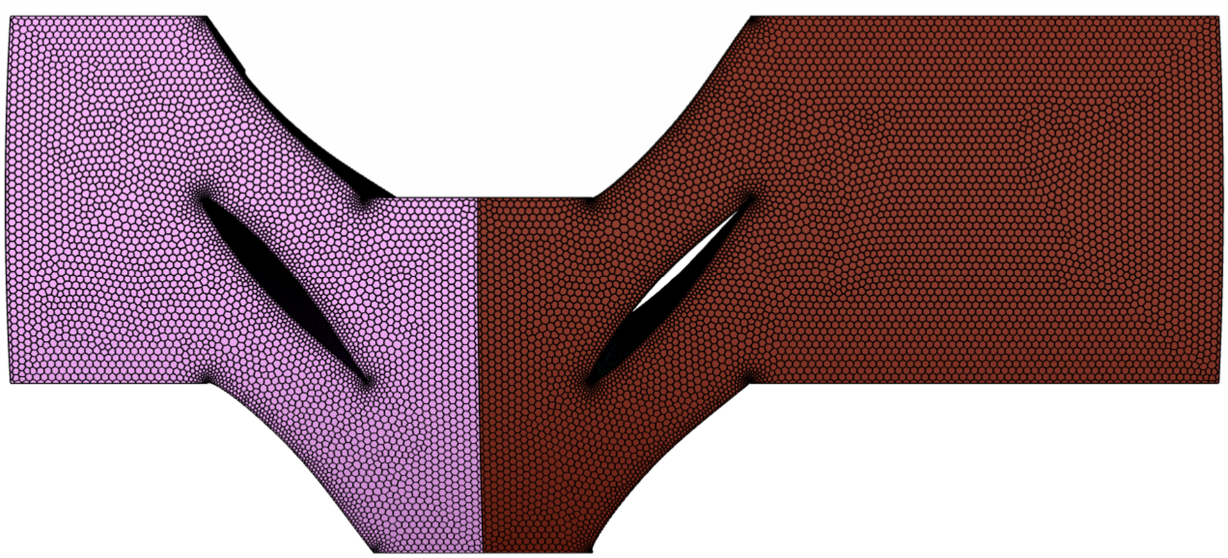

Figure 16: Mesh of the blades and air

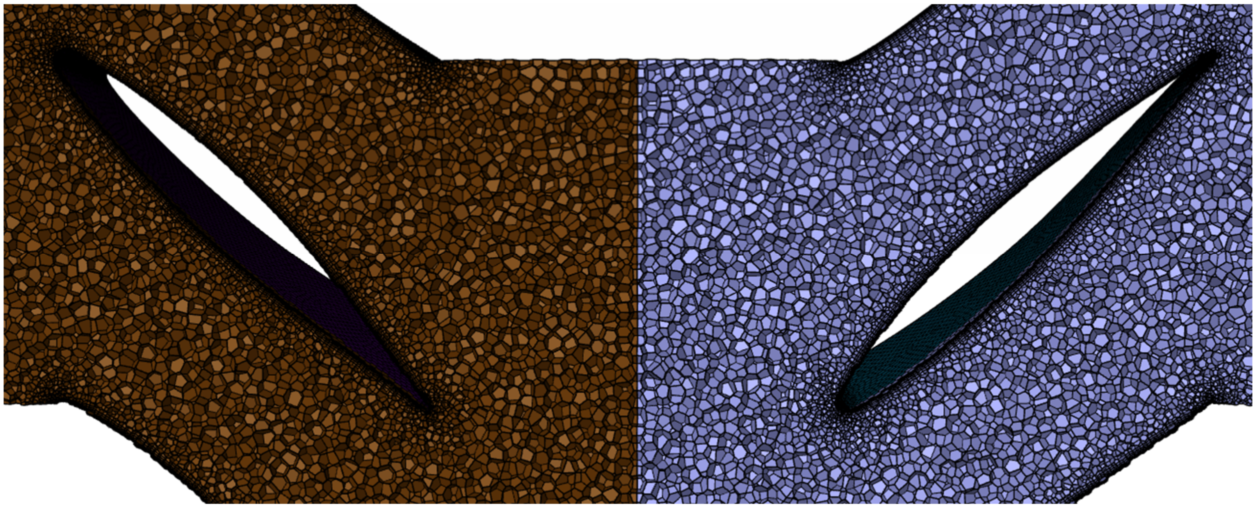

Figure 17: Boundary layers surrounding each blade

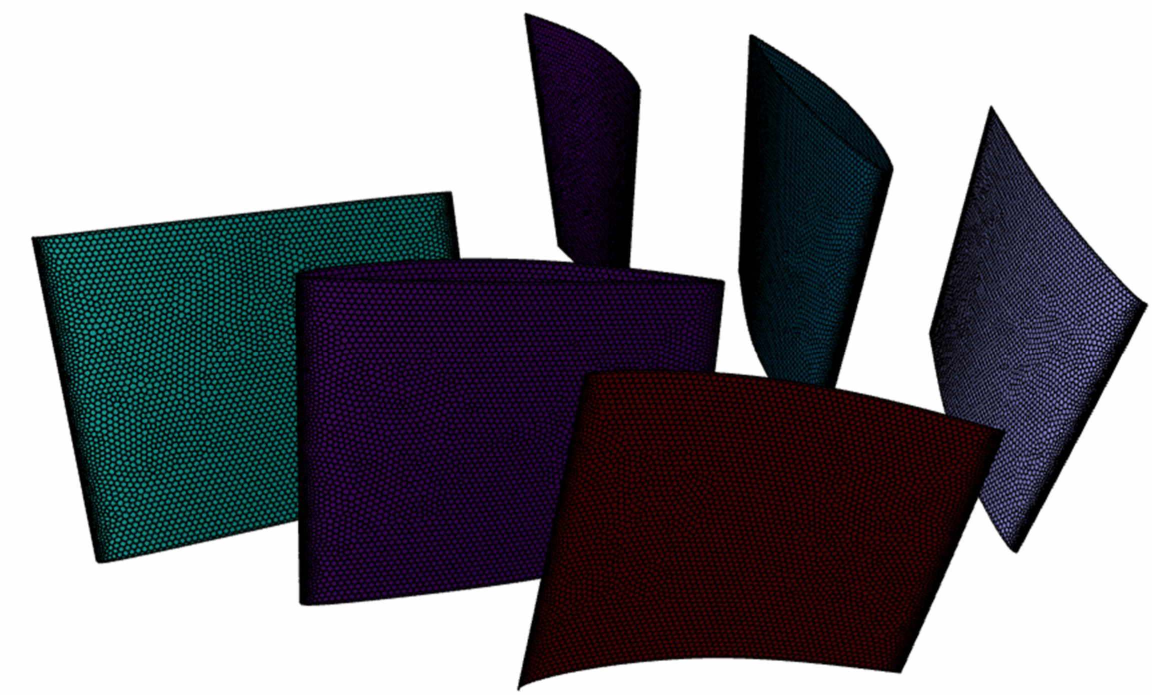

Figure 18: Mesh of blade surface

Material Properties:
The properties for air are calculated for air at 37,000'. The necessary initial conditions are discussed in the *Hand Calculations* section of the report. Given that problem inherently models compressible flow, the ideal gas law is used for the density of air.

Boundary Condition and Solver Settings:
The model is defined as a pressure-based transient model. The energy equation is turned on to allow for changes in temperature, and a realizable k-epsilon with scalable wall treatment

turbulence model is applied. For this simulation, the operating conditions set pressure to the outlet pressure of the stage (13.51 psi). The inlet duct is set as a pressure inlet and the outlet duct is set as a pressure outlet.

Rotational periodic boundary conditions are applied to the sides of the model to simulate the entire stage. A mesh interface with periodic repeats is used between the rotor and stator. All other boundaries are treated as non-slip walls. The stator cell zone does not move in the absolute reference frame. The rotor cell zone was given a rotational speed of 6,000 RPM. All simulations are allowed to run for 720 time steps with 10 iterations per time step with a time step size of $4.167*10^{-5}$ s using the Coupled solver with standard initialization based on the inlet. Convergence is monitored through monitors for mass flow rate, absolute pressure, and axial velocity at the inlet, outlet, and interface. A summary of the boundary conditions and solver settings is provided in the table below:

Table 10: Eighth Stage Model Boundary Conditions and Solver Settings

Parameter	Value
Inlet gauge total pressure	0.4227 psi
Inlet initial gauge pressure	-2.2515 psi
Inlet turbulent intensity	3.38%
Inlet turbulent length scale	0.0046 ft
Inlet total temperature	600 R
Outlet gauge pressure	0 psi
Reference pressure	13.51 psi
Outlet turbulent intensity	3.39%
Outlet turbulent length scale	0.0040 ft
Outlet total temperature	630 R
Rotor rotational speed	6,000 RPM
Pressure-velocity coupling scheme	Coupled
Gradient discretization method	Least Squares Cell Based
Pressure discretization method	Second Order
Momentum discretization method	Second Order Upwind
Turbulent kinetic energy discretization method	Second Order Upwind
Turbulent dissipation rate discretization method	Second Order Upwind
Energy discretization method	Second Order Upwind
Transient formulation	Second Order Implicit

Results:
After 720 time steps, all cases reach convergence. Residuals follow a regular sawtooth pattern dropping at least two orders of magnitude each time step, and the mass flow rate, absolute pressure, and axial velocity are stable.

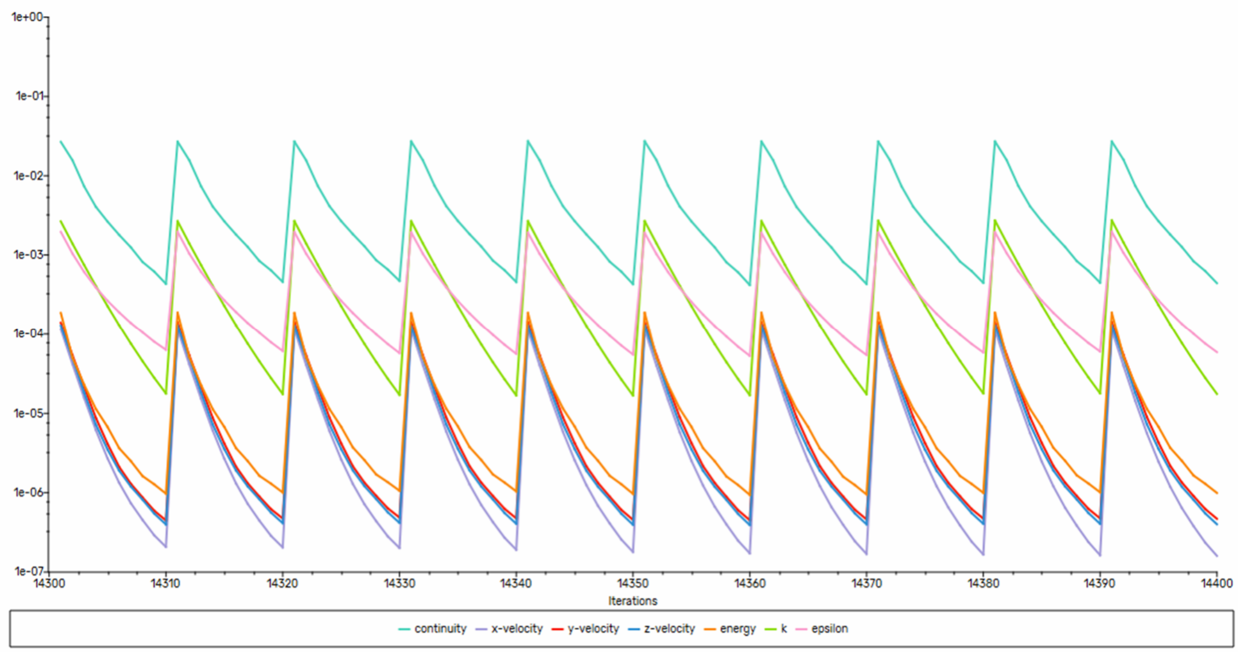

Figure 19: Plots of residuals

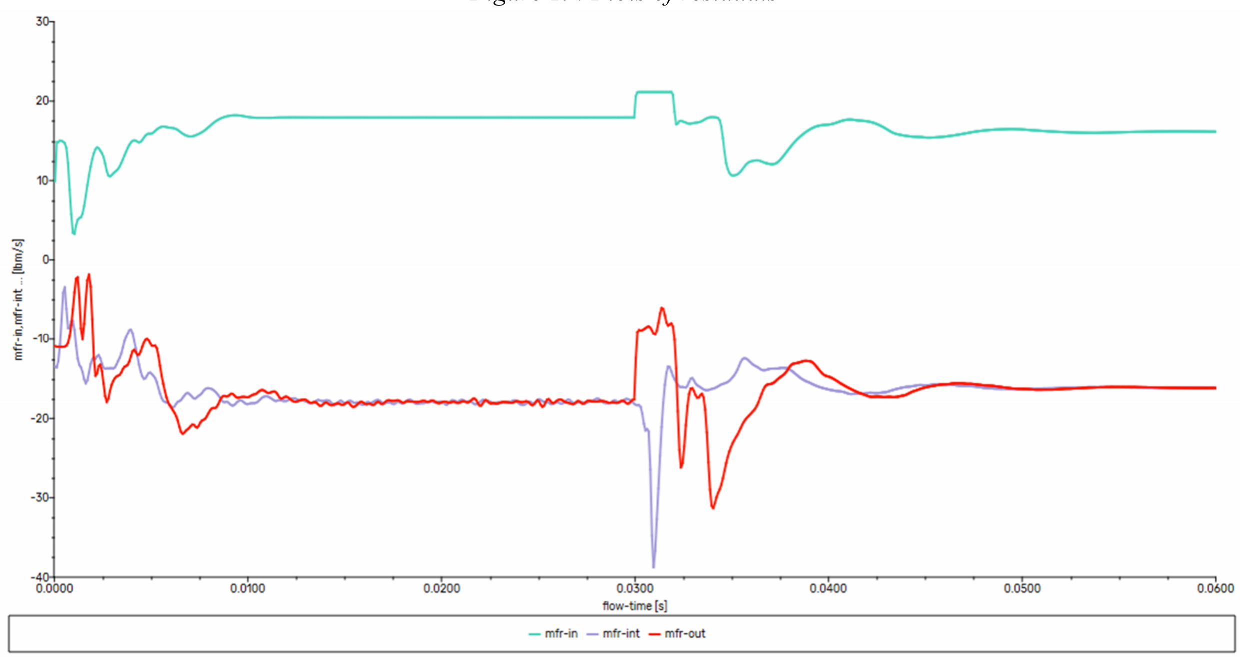

Figure 20: Convergence history for mass flow rate

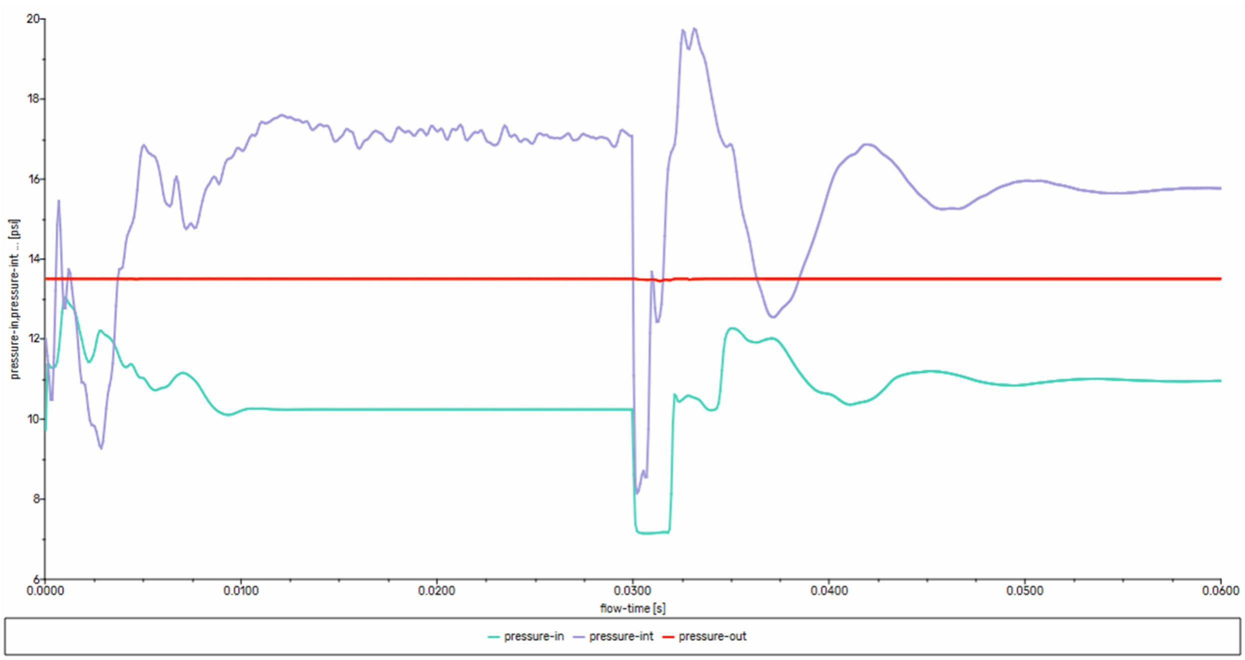

Figure 21: Convergence history for absolute pressure

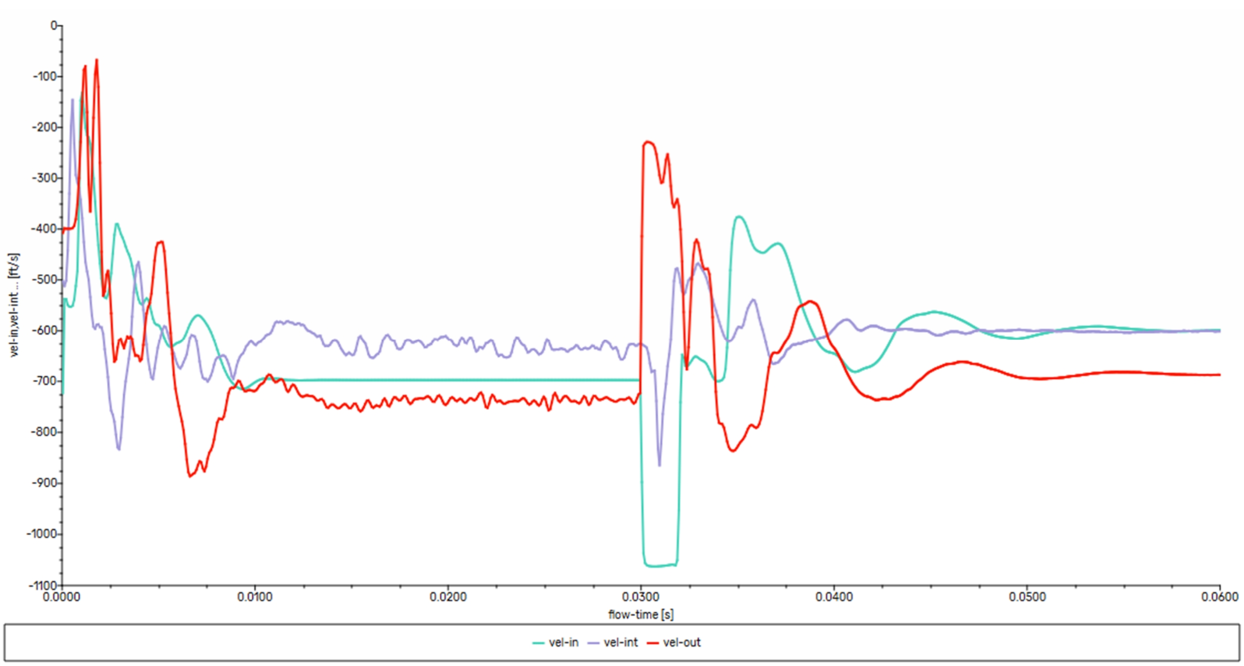

Figure 22: Convergence history of axial velocity

To visualize the behavior inside the compressor, contour plots of pressure and temperature and streamlines of velocity are shown below.

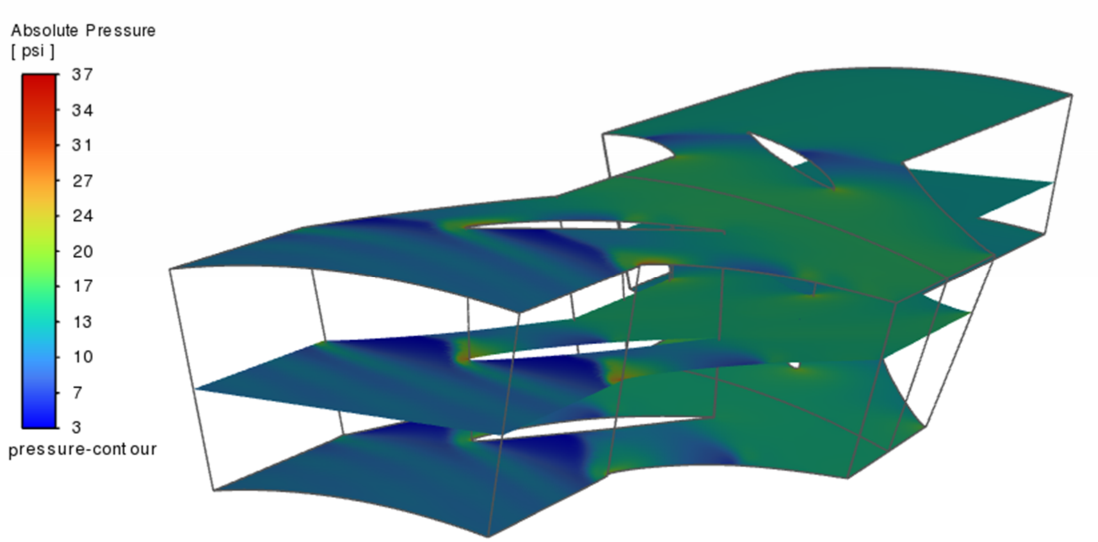

Figure 23: Pressure contour inside the eighth stage

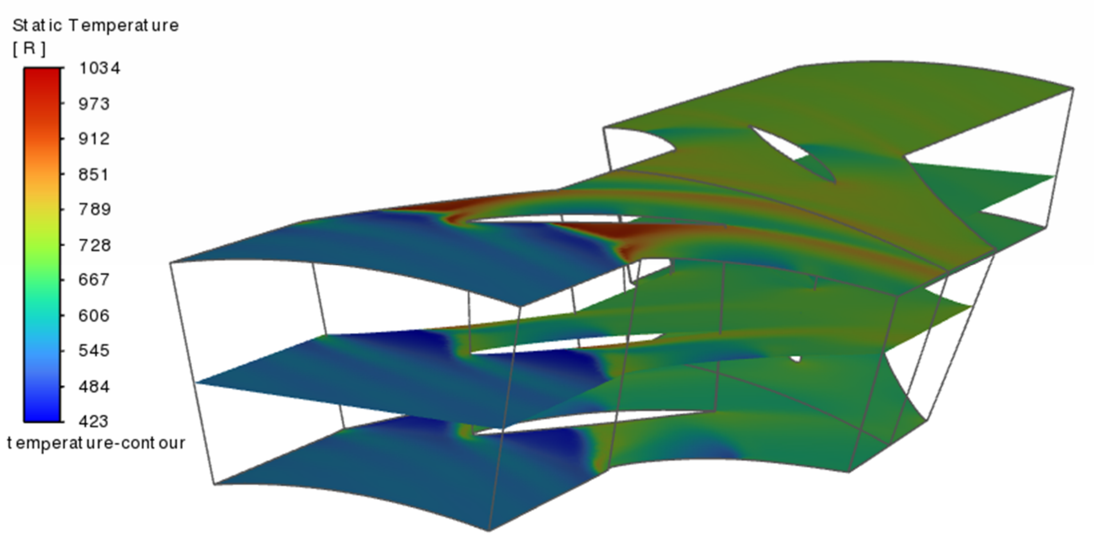

Figure 24: Temperature contour inside the eighth stage

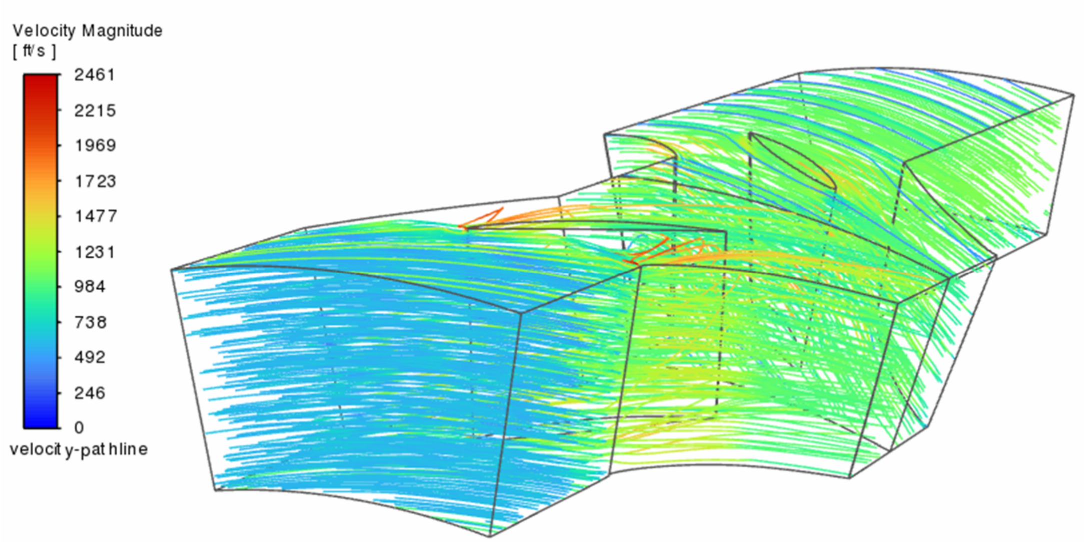

Figure 25: Velocity streamlines around the rotor and stator blades for the eighth stage

Table 11: Summary of the results for the eighth stage

Parameter	Value
Mass flow rate	16.16 lb/s
Inlet pressure	10.95 psi
Outlet pressure	13.51 psi
Inlet temperature	559 R
Outlet temperature	686 R
Specific enthalpy change	34.20 BTU/lb
Pressure ratio	1.23

Hand Calculations for Validation:

These results are mostly validated by comparison to the theoretical values computed in the hand calculations above. To calculate the overall mass flow rate, we simply multiply the mass flow rate of the segment by the number of 21.18° segments in a 360° compressor (17). To calculate the actual exit temperature, we use the following formula:

$$T_{2,actual} = T_1 + \frac{w_{actual}}{c_p}$$

A summary of the simulation values compared to the hand calculation values is provided in the table below:

Table 12: Comparison of eighth stage results to hand calculations

Parameter	**Simulation Value**	**Hand Calculation Value**
Total mass flow rate	16.16*17 segments = 274.72 lb/s	250.08 lb/s
Inlet pressure	10.95 psi	11.26 psi
Outlet pressure	13.51 psi	13.51 psi
Inlet temperature	559 R	562 R
Outlet temperature	686 R	723 R
Specific enthalpy change	34.20 BTU/lb	38.73 BTU/lb
Pressure ratio	1.23	1.2

Compressor Design: Final Stage Model

Motivation:
As is discussed in the *Design Concept and Assumptions*, the primary purpose of this model is help verify the governing hand calculations used to characterize the compressor. Using the same initial conditions as are in these calculations, pressure, temperature, and velocity is better characterized in the compressor, and the hand calculations are effectively validated.

Geometry and Mesh:
The geometry of the final stage consists of a set of rotor blades, a set of stator blades, and inlet and outlet ducts. We chose to use a set of three blades for each half of the stage (one full blade in the middle and half of a blade on either end of the model) to allow for rotationally periodic conditions to be easily applied. As both the rotor and stator in this stage consists of 36 blades, a 20° model is created to cut the overall cell count down. For these studies, the blades are modeled implicitly (assuming the blades do not directly transfer heat to the air or vice versa). A polyhedral mesh is used to ensure good quality cells around the blades. A summary of meshing parameters and the resulting geometry is shown below:

Table 13: Final Stage Model Meshing Parameters

Meshing Parameter	Value
Blade local sizing	0.25 in.
Air local sizing	0.5 in.
Number of blade boundary layers	5
Volume mesh size	0.5 in.
Volume mesh growth rate	1.2
Total number of cells	657,730

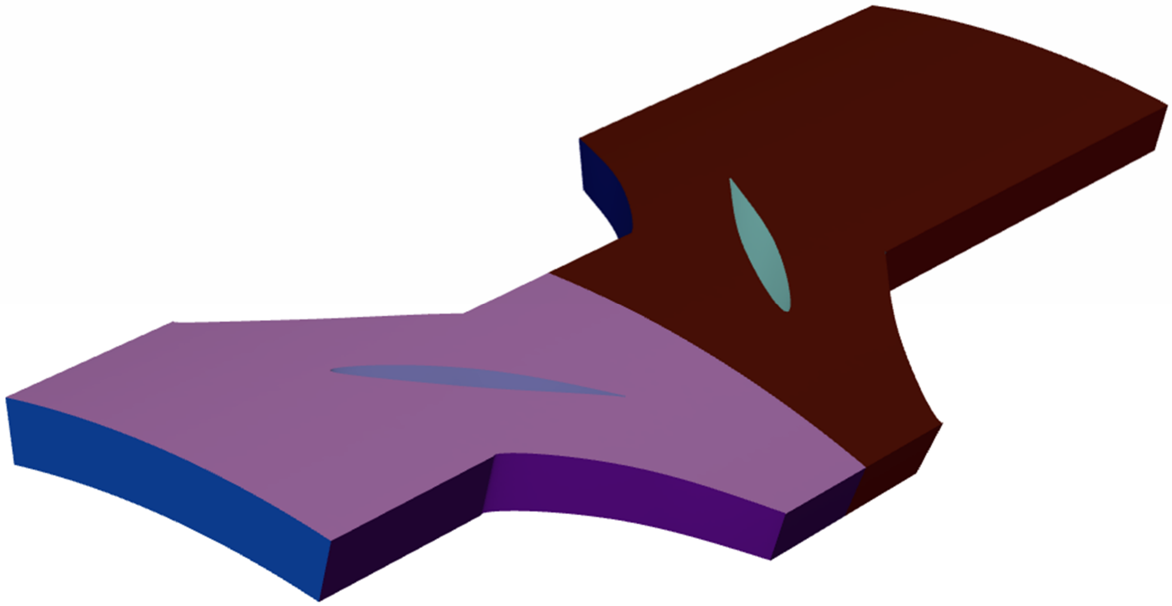

Figure 26: Geometry of the final stage model

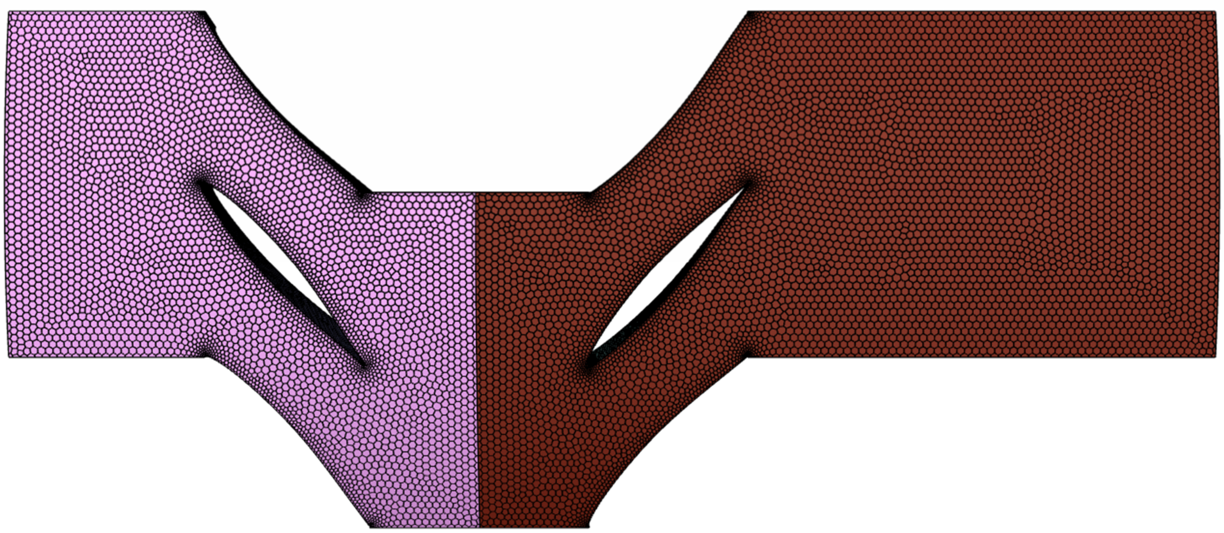

Figure 27: Mesh of the blades and air

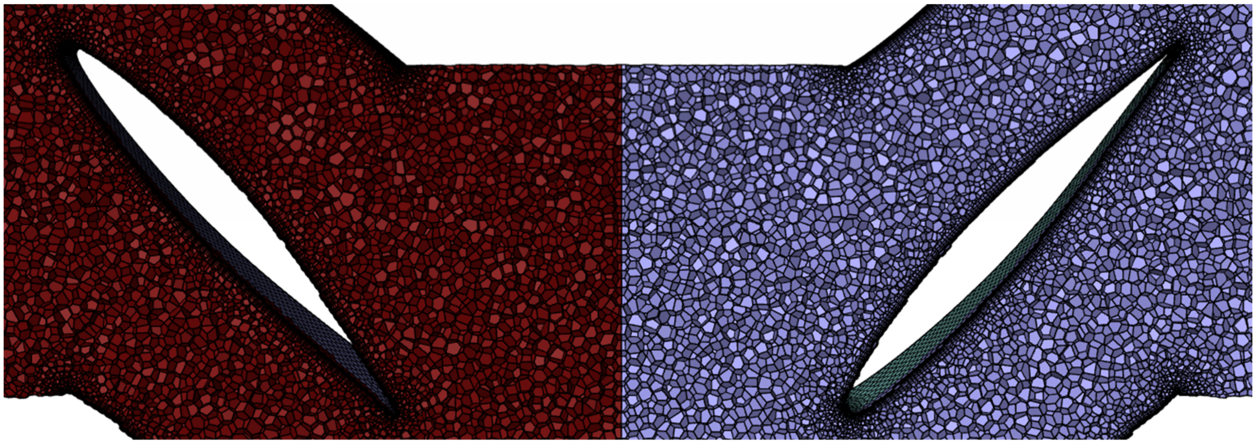

Figure 28: Boundary layers surrounding each blade

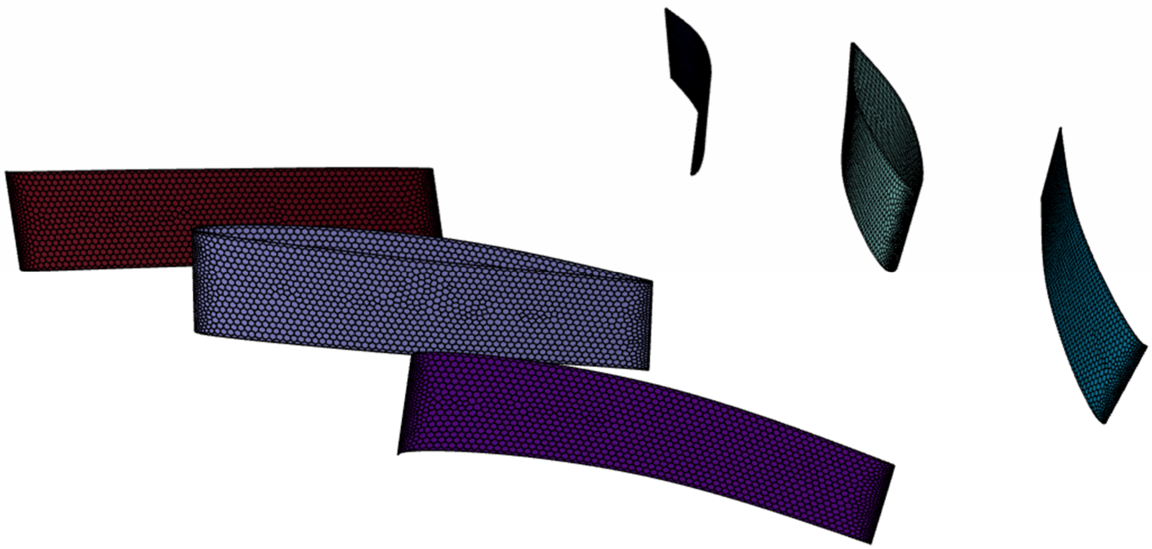

Figure 29: Mesh of blade surface

Material Properties:
The properties for air are calculated for air at 37,000'. The necessary initial conditions are discussed in the *Hand Calculations* section of the report. Given that problem inherently models compressible flow, the ideal gas law is used for the density of air.

Boundary Condition and Solver Settings:
The model is defined as a pressure-based transient model. The energy equation is turned on to allow for changes in temperature, and a realizable k-epsilon with scalable wall treatment turbulence model is applied. For this simulation, the operating conditions set pressure to the outlet pressure of the stage (69.70 psi). The inlet duct is set as a pressure inlet and the outlet duct is set as a pressure outlet.

Rotational periodic boundary conditions are applied to the sides of the model to simulate the entire stage. A mesh interface with periodic repeats is used between the rotor and stator. All other boundaries are treated as non-slip walls. The stator cell zone does not move in the absolute reference frame. The rotor cell zone was given a rotational speed of 6,000 RPM. All simulations are allowed to run for 720 time steps with 10 iterations per time step with a time step size of $4.167*10^{-5}$ s using the Coupled solver with standard initialization based on the inlet. Convergence is monitored through monitors for mass flow rate, absolute pressure, and axial velocity at the inlet, outlet, and interface. A summary of the boundary conditions and solver settings is provided in the table below:

Table 14: Final Stage Model Boundary Conditions and Solver Settings

Parameter	Value
Inlet gauge total pressure	-2.9831 psi
Inlet initial gauge pressure	-11.6174 psi
Inlet turbulent intensity	3.44%
Inlet turbulent length scale	0.0012 ft
Inlet total temperature	936 R
Outlet gauge pressure	0 psi
Reference pressure	69.70 psi
Outlet turbulent intensity	3.50%
Outlet turbulent length scale	0.0011 ft
Outlet total temperature	984 R
Rotor rotational speed	6,000 RPM
Pressure-velocity coupling scheme	Coupled
Gradient discretization method	Least Squares Cell Based
Pressure discretization method	Second Order
Momentum discretization method	Second Order Upwind
Turbulent kinetic energy discretization method	Second Order Upwind
Turbulent dissipation rate discretization method	Second Order Upwind
Energy discretization method	Second Order Upwind
Transient formulation	Second Order Implicit

Results:
After 720 time steps, all cases reach convergence. Residuals follow a regular sawtooth pattern dropping at least two orders of magnitude each time step, and the mass flow rate, absolute pressure, and axial velocity are stable.

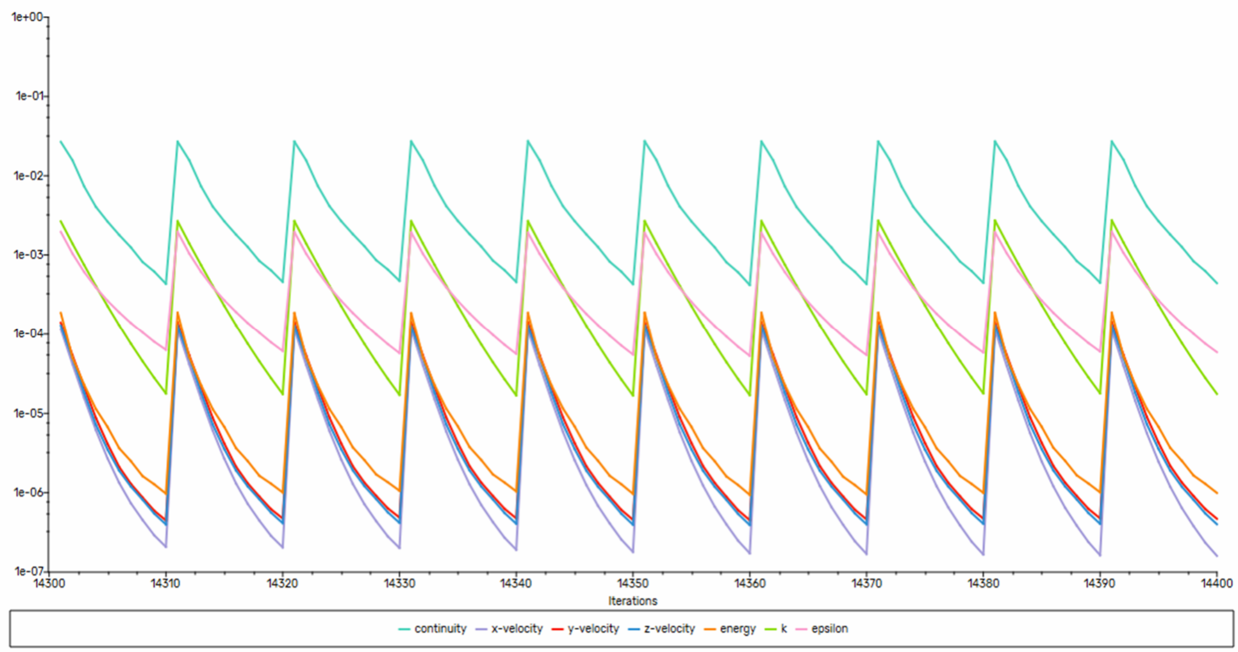

Figure 30: Plots of residuals

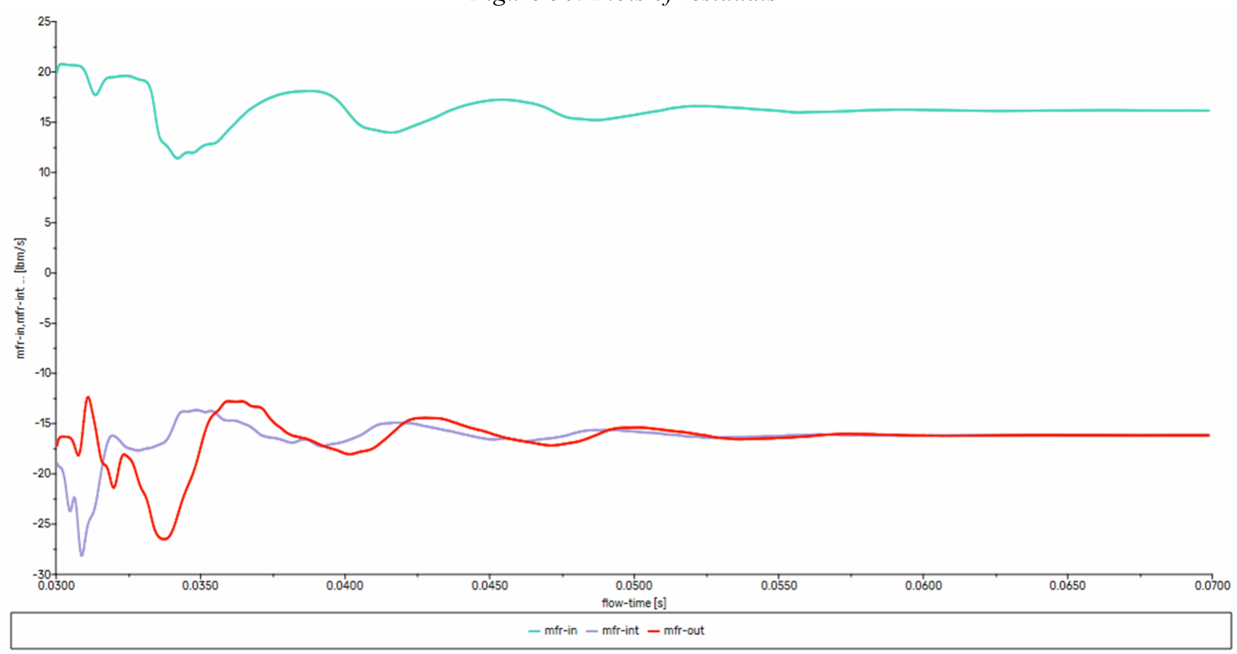

Figure 31: Convergence history for mass flow rate

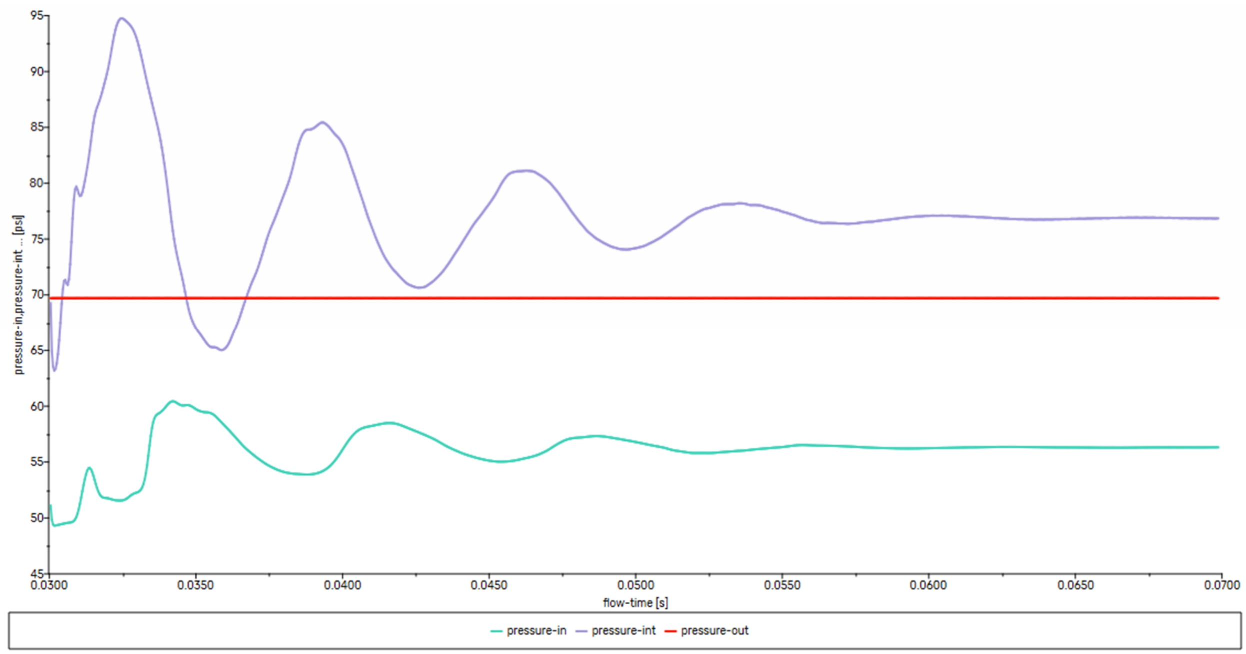

Figure 32: Convergence history for absolute pressure

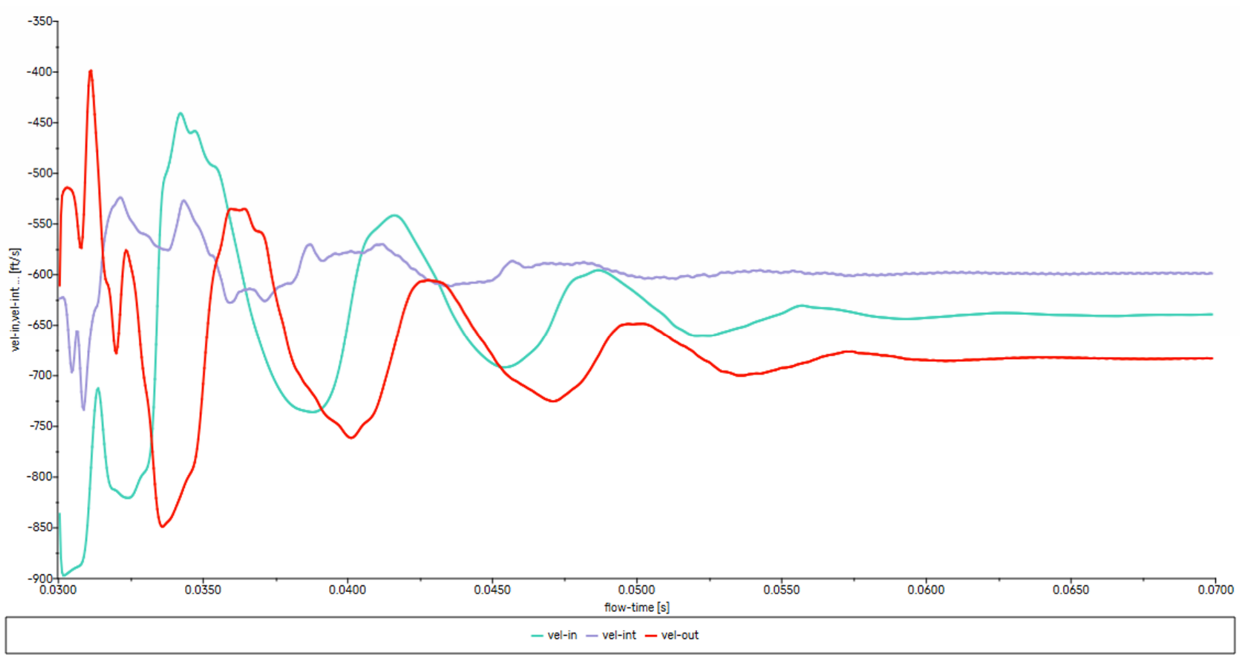

Figure 33: Convergence history of axial velocity

To visualize the behavior inside the compressor, contour plots of pressure and temperature and streamlines of velocity are shown below.

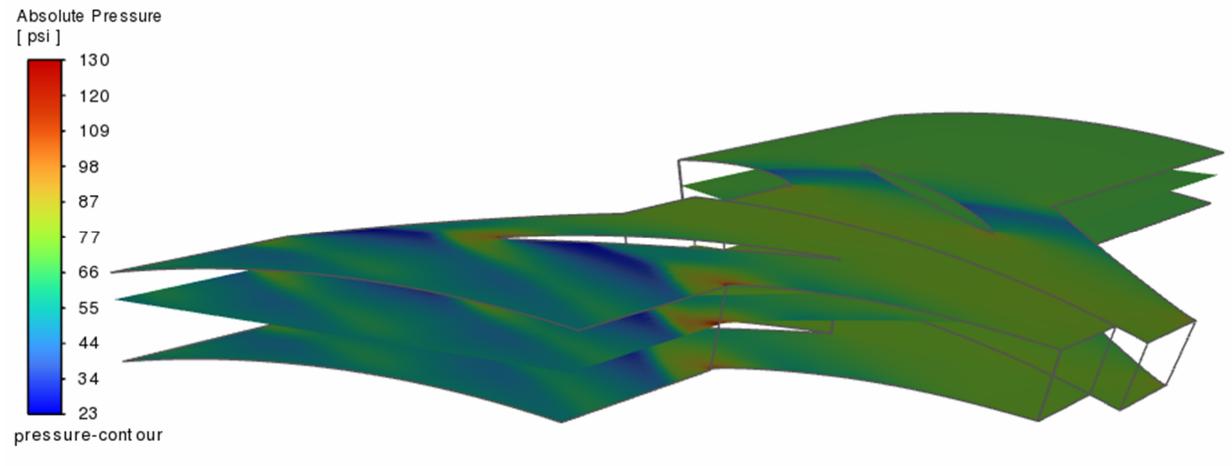

Figure 34: Pressure contour inside the final stage

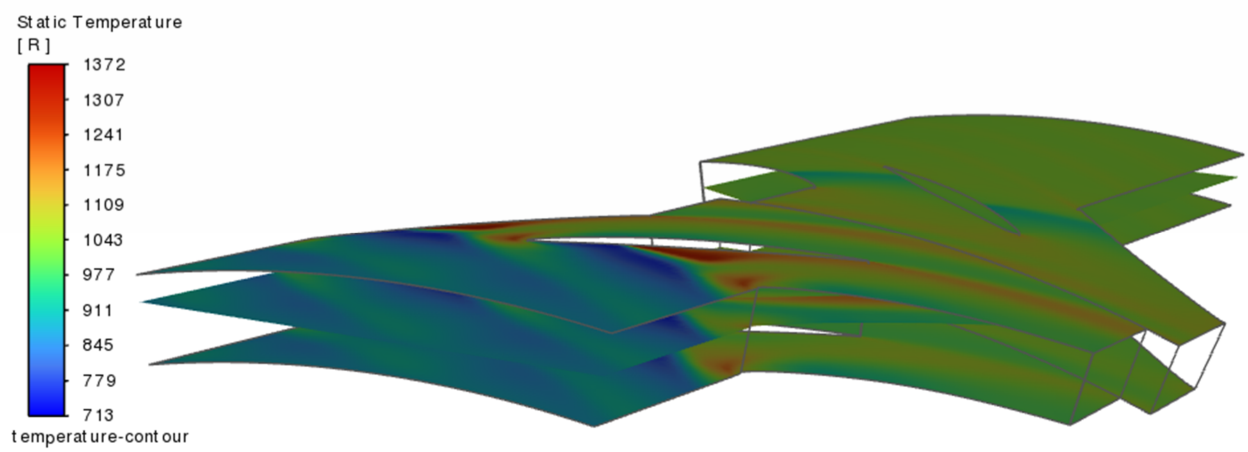

Figure 35: Temperature contour inside the final stage

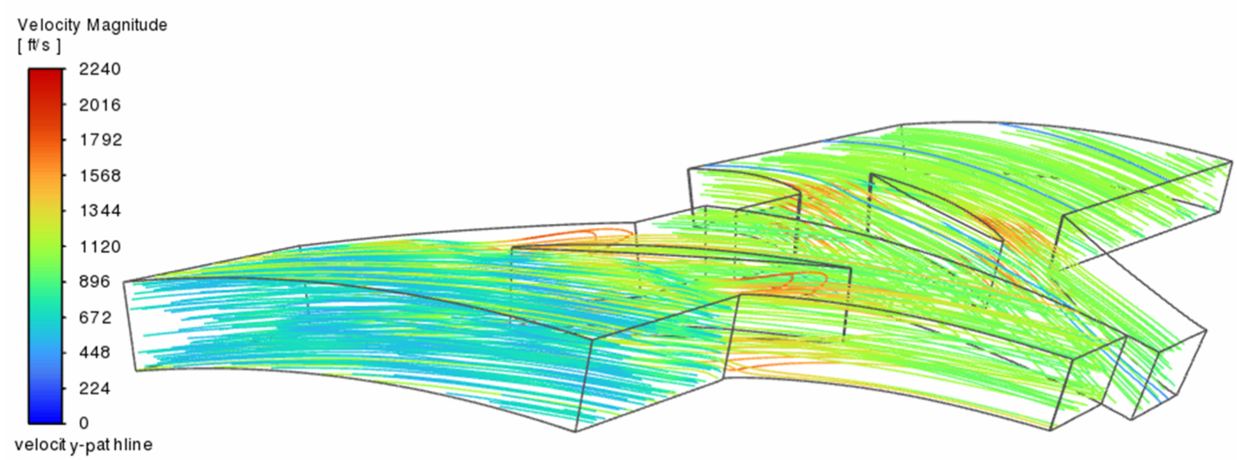

Figure 36: Velocity streamlines around the rotor and stator blades for the final stage

Table 15: Summary of the results for the final stage

Parameter	Value
Mass flow rate	16.16 lb/s
Inlet pressure	56.32 psi
Outlet pressure	69.70 psi
Inlet temperature	891 R
Outlet temperature	1,035 R
Specific enthalpy change	37.02 BTU/lb
Pressure ratio	1.24

Hand Calculations for Validation:

These results are mostly validated by comparison to the theoretical values computed in the hand calculations above. To calculate the overall mass flow rate, we simply multiply the mass flow rate of the segment by the number of 20° segments in a 360° compressor (18). To calculate the actual exit temperature, we use the following formula:

$$T_{2,actual} = T_1 + \frac{w_{actual}}{c_p}$$

A summary of the simulation values compared to the hand calculation values is provided in the table below:

Table 16: Comparison of final stage results to hand calculations

Parameter	Simulation Value	Hand Calculation Value
Total mass flow rate	16.16*18 segments = 290.88 lb/s	250.08 lb/s
Inlet pressure	56.32 psi	58.09 psi
Outlet pressure	69.70 psi	69.70 psi
Inlet temperature	891 R	897 R
Outlet temperature	1,035 R	1,069 R
Specific enthalpy change	37.02 BTU/lb	41.21 BTU/lb
Pressure ratio	1.24	1.2

Design Summary

The final compressor design attains the required compression ratio in 17 stages. The design features optimization on the swept blade angle of the rotor blades. The CFD simulations were performed to compare results between the hand calculations and k-epsilon turbulence model. The simulations were performed for various rotational speeds and geometries to attain an ideal overall performance for the compressor. The average compressor efficiency is 78% and yields an average compression ratio of 1.2 per stage. The compressor consumes 283,573 hp at 37,000 feet and 980,845 hp at ground level.

Design Time Estimate:
250 hours total

Scaled Drawings (all dimensions in feet):

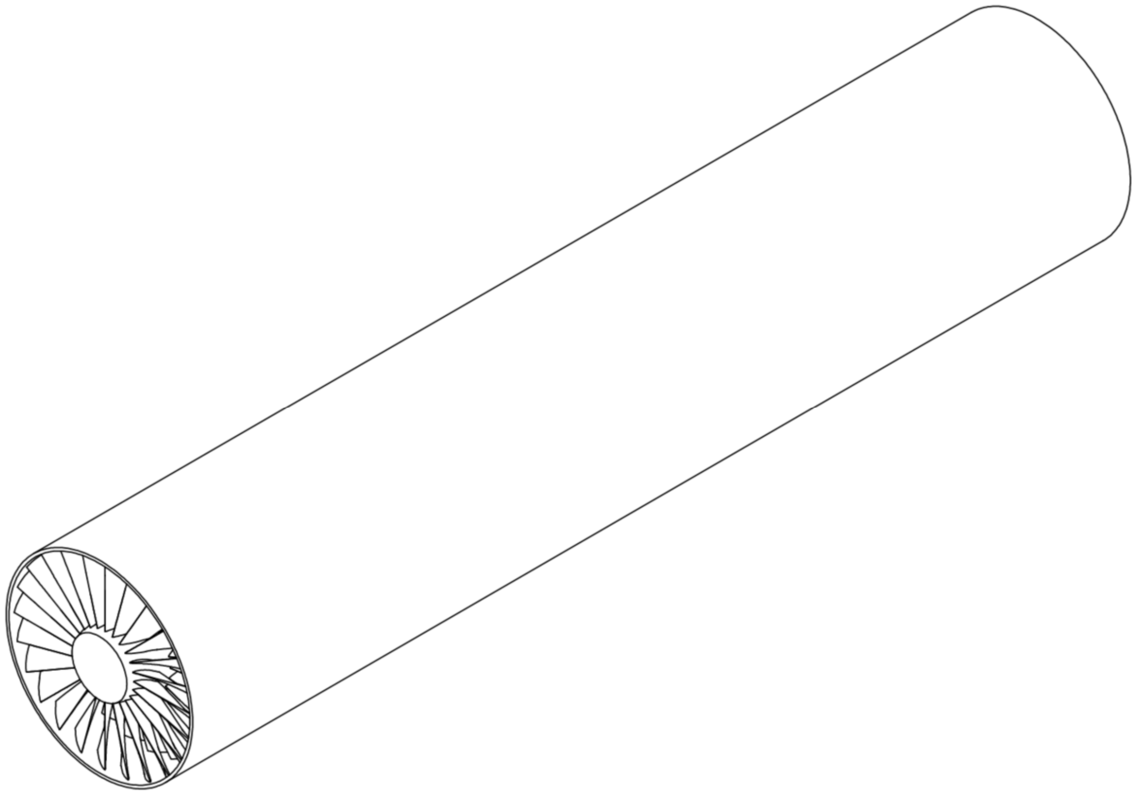

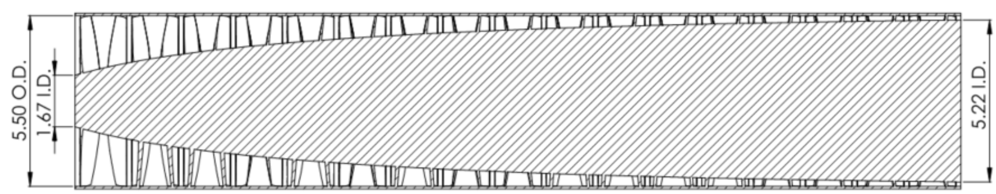

SECTION A-A
SCALE 1 : 20

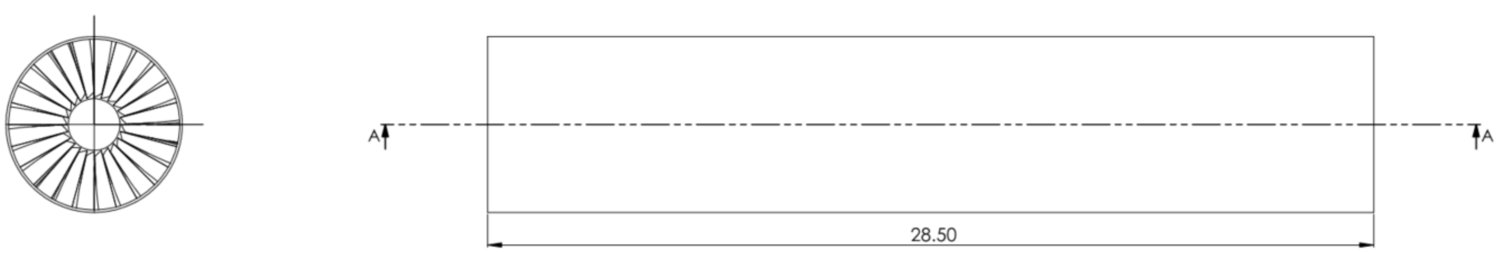

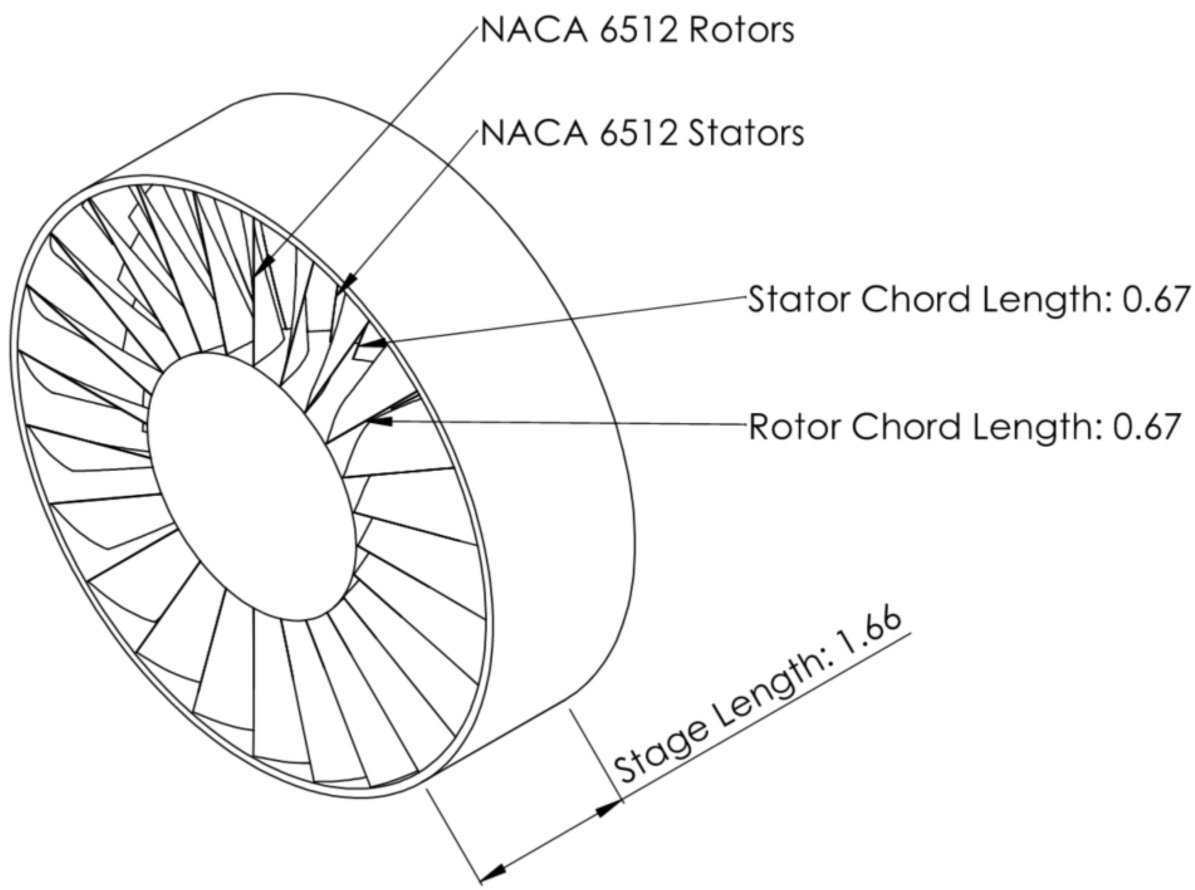
NACA 6512 Rotors
NACA 6512 Stators
Stator Chord Length: 0.67
Rotor Chord Length: 0.67
Stage Length: 1.66

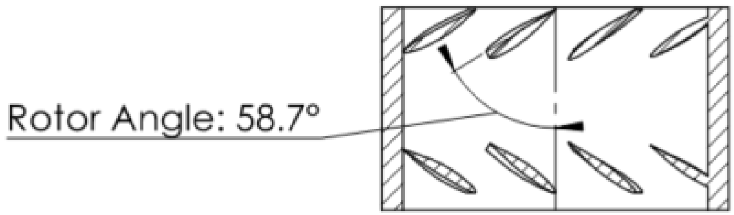

Shroud
SECTION B-B

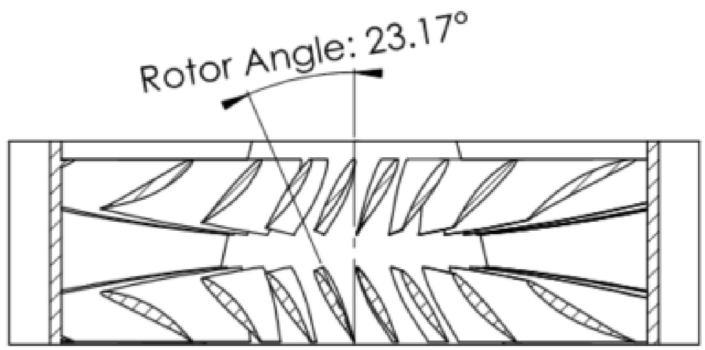

Hub
SECTION A-A

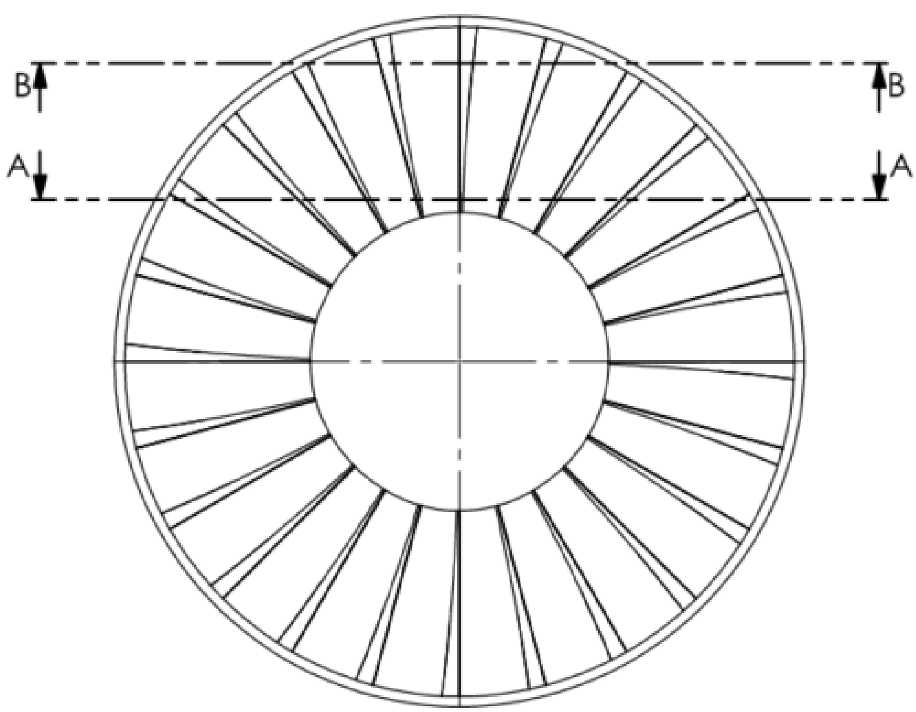

Citations

1. Wright, L. C. "Blade Selection for a Modern Axial-Flow Compressor." *Conference Proceedings of Pennsylvania State Univ. Fluid Mech., Acoustics, and Design of Turbomachinery, Pt. 2*, 1974.

2. Boyce, M.P. *Gas Turbine Engineering Handbook, Second Edition*, Butterworth-Hienemann, 2003.

3. "U.S. Standard Atmosphere, 1976." *Technical Memorandum*, NOAA-S/T-76-1562; NASA-TM-X-74335, October 1, 1976. Public.

4. "Details for Airfoil (NACA 651212)." *Airfoil Tools*, http://airfoiltools.com/airfoil/details?airfoil=naca651212-il.

5. Wikipedia Contributors. "Axial Compressor." *Wikipedia, The Free Encyclopedia*, Wikipedia Foundation, https://en.wikipedia.org/wiki/Axial_compressor.

Properties of Air at STP		
Pressure	14.69594878	psi
Temperature	518.69	R
Density	0.076474252	lb/ft^3
Viscosity	1.20242E-05	lb/ft-s
Thermal Conductivity	1.46637E-05	BTU/hr-ft-R
Specific Heat Capacity	0.24	BTU/lb-R

Properties of Air at 37,000' (11277.6 m)		
Pressure	3.14180747	psi
Temperature	389.99	R
Density	0.021745532	lb/ft^3
Viscosity	9.55E-06	lb/ft-s
Thermal Conductivity	1.12935E-05	BTU/hr-ft-R
Specific Heat Capacity	0.24	BTU/lb-R

Turbulence Properties		
First Stage Inlet		
Dh	3.833333333	in
Re	4.92E+05	
Ti	0.031088	
L	0.022361111	ft
First Stage Outlet		
Dh	3.023650416	in
Re	4.42E+05	
Ti	0.031507	
L	0.017637961	ft
Eighth Stage Inlet		
Dh	0.788695343	in
Re	2.52E+05	
Ti	0.033802	
L	0.004600723	ft
Eighth Stage Outlet		
Dh	0.681958302	in
Re	2.48E+05	
Ti	0.033866	
L	0.00397809	ft
Last Stage Inlet		
Dh	0.213456947	in
Re	2.20E+05	
Ti	0.034376	
L	0.001245166	ft
Last Stage Outlet		
Dh	0.186690684	in
Re	1.93E+05	
Ti	0.034957	
L	0.001089029	ft

Boundary Conditions		
First Stage		
Inlet Total Temperature	428.1054131	R
Outlet Total Temperature	448.9591628	R
Inlet Stagnation Pressure	0.446367598	psi
Inlet Initial Pressure	-0.62836149	psi
Eighth Stage		
Inlet Total Temperature	599.7010131	R
Outlet Total Temperature	629.7304127	R
Inlet Stagnation Pressure	0.422737053	psi
Inlet Initial Pressure	-2.25153284	psi
Last Stage		
Inlet Total Temperature	935.5956247	R
Outlet Total Temperature	983.5861569	R
Inlet Stagnation Pressure	-2.98310702	psi
Inlet Initial Pressure	-11.6174149	psi

PRESSURE RATIO CALCULATION (37,000')

Stage	1	2	3	4	5	6	7	8	9	10	11	12	13	14	15	16	17	End of 17
Inlet Pressure (psi)	3.14180747	3.770168964	4.524202757	5.429043308	6.51485197	7.817822364	9.381386837	11.2576642	13.50919704	16.21103645	19.45324374	23.34389249	28.01267099	33.61520519	40.33824623	48.40589547	58.08707457	69.7044895
Inlet Temperature (R)	389.99	410.8437497	432.812602	455.9561843	480.3373124	506.0221609	533.0804431	561.5856	591.6149996	623.2501469	656.5769054	691.6857298	728.6719117	767.6358381	808.683264	851.9255994	897.4802115	945.470744
Density (lb/ft^3)	0.021745532	0.024770117	0.028215392	0.032139871	0.036610205	0.041702318	0.047502692	0.054109841	0.061635978	0.070208925	0.079974283	0.091097905	0.103768711	0.118201899	0.134642599	0.153370036	0.174702272	0.19900161
Mass Flow Rate (lb/s)	317.6452519	317.6452519	317.6452519	317.6452519	317.6452519	317.6452519	317.6452519	317.6452519	317.6452519	317.6452519	317.6452519	317.6452519	317.6452519	317.6452519	317.6452519	317.6452519	317.6452519	
OD (in)	66	66	66	66	66	66	66	66	66	66	66	66	66	66	66	66	66	66
ID (in)	20	29.716195	36.15412566	40.98058011	44.79103159	47.88692172	50.44842139	52.59441344	54.40864075	55.95287151	57.27423229	58.40961183	59.38846498	60.23468342	60.96789249	61.6043793	62.15777496	62.6395677
RPM	6000	6000	6000	6000	6000	6000	6000	6000	6000	6000	6000	6000	6000	6000	6000	6000	6000	
U (fps)	1125.737368	1252.922063	1337.194378	1400.372519	1450.251212	1490.776319	1524.306271	1552.397242	1576.145422	1596.359355	1613.655927	1628.518011	1641.331168	1652.408142	1662.005826	1670.337419	1677.581351	
Vf (fps)	677	677	677	677	677	677	677	677	677	677	677	677	677	677	677	677	677	
Vw1 (fps)	1125.737368	1252.922063	1337.194378	1400.372519	1450.251212	1490.776319	1524.306271	1552.397242	1576.145422	1596.359355	1613.655927	1628.518011	1641.331168	1652.408142	1662.005826	1670.337419	1677.581351	
beta1 (rad)	1.029360089	1.075402275	1.102134235	1.120482004	1.134046812	1.144516678	1.152829205	1.159561808	1.165095928	1.169696731	1.173555844	1.176816036	1.179586316	1.181951605	1.183979172	1.185723055	1.187227181	
beta2 (rad)	0.72752277	0.78446582	0.83423819	0.86230483	0.89019758	0.91145478	0.92794748	0.94024524	0.95116939	0.96355454	0.96817203	0.98061709	0.98565949	0.99155487	0.9959322	0.99993912	1.00333425	
Vw2 (fps)	522.8917495	577.1832801	590.6112023	610.3237172	614.0896501	617.284722	620.411922	624.9480414	627.0967946	622.0079472	629.6390467	617.7915701	619.498526	617.3742196	617.0149989	616.1135614	1062.137801	
Blade angle (rad)	0.261799388	0.235224011	0.220399785	0.210456396	0.20321814	0.197693879	0.193345235	0.18984661	0.186986143	0.184618427	0.182639526	0.180972732	0.179559957	0.178356271	0.177326306	0.176441808	0.175679918	
Blade spacing (in)	5.628686838	5.628686838	5.628686838	5.628686838	5.628686838	5.628686838	5.628686838	5.628686838	5.628686838	5.628686838	5.628686838	5.628686838	5.628686838	5.628686838	5.628686838	5.628686838	5.628686838	
Number of blades	24	27	29	30	31	32	33	34	34	35	35	35	35	36	36	36	36	
Blade solidity	1.421290655	1.421290655	1.421290655	1.421290655	1.421290655	1.421290655	1.421290655	1.421290655	1.421290655	1.421290655	1.421290655	1.421290655	1.421290655	1.421290655	1.421290655	1.421290655	1.421290655	
Power (hp)	10557.72839	12970.58046	14165.04099	15329.41	15973.37282	16505.15575	16961.87993	17400.76681	17727.70348	17809.35573	18223.18162	18044.96971	18237.19776	18297.31774	18392.88589	18458.08289	18517.97221	
w_stage_ideal (BTU/lb)	5.004899925	5.272524557	5.554459754	5.851470737	6.164363648	6.493987731	6.841237647	7.207055892	7.592435363	7.998422046	8.426117862	8.876683652	9.351342333	9.851382212	10.37816049	10.93310692	11.51772775	
w_stage_actual (BTU/lb)	23.49705335	28.86704506	31.52541072	34.11680536	35.54999519	36.73351985	37.74999535	38.72677257	39.4543958	39.63611927	40.55712129	40.16049668	40.5883153	40.72211703	40.93481147	41.0799125	41.21320089	
Stage Efficiency	0.783001173	0.752648572	0.746189925	0.741512856	0.743399845	0.746786427	0.751224861	0.756100091	0.762435728	0.771796296	0.777759269	0.791030226	0.800394937	0.811917241	0.823528967	0.83614241	0.849466955	
Pressure ratio	1.2	1.2	1.2	1.2	1.2	1.2	1.2	1.2	1.2	1.2	1.2	1.2	1.2	1.2	1.2	1.2	1.2	
Cumulative pressure ratio	1.2	1.44	1.728	2.0736	2.48832	2.985984	3.5831808	4.29981696	5.159780352	6.191736422	7.430083707	8.916100448	10.69932054	12.83918465	15.40702157	18.48842589	22.18611107	

Total power: 283572.6 hp

PRESSURE RATIO CALCULATION (STP)

Stage	1	2	3	4	5	6	7	8	9	10	11	12	13	14	15	16	17	End of 17
Inlet Pressure (psi)	14.69594878	17.63513854	21.16216624	25.39459949	30.47351939	36.56822327	43.88186792	52.65824151	63.18988981	75.82786777	90.99344132	109.1921296	131.0305555	157.2366666	188.6839999	226.4207999	271.7049599	326.045952
Inlet Temperature (R)	518.69	546.4256635	575.644423	606.4255833	638.85269	673.0137559	709.0015002	746.9136	786.8529555	828.9279692	873.25284	919.9478736	969.1398084	1020.96216	1075.555584	1133.068256	1193.656276	1257.48409
Density (lb/ft^3)	0.076474252	0.087111054	0.09922733	0.113028857	0.128750039	0.14665788	0.167056522	0.190292411	0.216760179	0.246909349	0.281251966	0.320371297	0.364931736	0.415690085	0.473508411	0.539368689	0.61438947	0.69984489
Mass Flow Rate (lb/s)	1150.089631	1150.089631	1150.089631	1150.089631	1150.089631	1150.089631	1150.089631	1150.089631	1150.089631	1150.089631	1150.089631	1150.089631	1150.089631	1150.089631	1150.089631	1150.089631	1150.089631	
OD (in)	66	66	66	66	66	66	66	66	66	66	66	66	66	66	66	66	66	66
ID (in)	20	29.716195	36.15412566	40.98058011	44.79103159	47.88692172	50.44842139	52.59441344	54.40864075	55.95287151	57.27423229	58.40961183	59.38846498	60.23468342	60.96789249	61.6043793	62.15777496	62.6395677
RPM	6000	6000	6000	6000	6000	6000	6000	6000	6000	6000	6000	6000	6000	6000	6000	6000	6000	
U (fps)	1125.737368	1252.922063	1337.194378	1400.372519	1450.251212	1490.776319	1524.306271	1552.397242	1576.145422	1596.359355	1613.655927	1628.518011	1641.331168	1652.408142	1662.005826	1670.337419	1677.581351	
Vf (fps)	697	697	697	697	697	697	697	697	697	697	697	697	697	697	697	697	697	
Vw1 (fps)	1125.737368	1252.922063	1337.194378	1400.372519	1450.251212	1490.776319	1524.306271	1552.397242	1576.145422	1596.359355	1613.655927	1628.518011	1641.331168	1652.408142	1662.005826	1670.337419	1677.581351	
alpha1 (rad)	1.016415005	1.063129466	1.090300988	1.108970609	1.122783628	1.133450911	1.141923735	1.148788445	1.154432663	1.159126021	1.16306348	1.166390362	1.169217669	1.171631908	1.173701626	1.175481901	1.17701752	
alpha2 (rad)	0.72752277	0.78446582	0.83423819	0.86230483	0.89019758	0.91145478	0.92794748	0.94024524	0.95116939	0.96355454	0.96817203	0.98061709	0.98565949	0.99155487	0.9959322	0.99993912	1.00333425	
Vw2 (fps)	505.0824255	557.2205392	568.5555693	586.9840185	589.3876837	591.4799481	593.708987	597.5492467	599.0599075	593.223563	600.5691241	587.9325911	589.3114465	586.7971466	586.143778	584.9695774	584.0657722	
Blade angle (rad)	0.261799388	0.235224011	0.220399785	0.210456396	0.20321814	0.197693879	0.193345235	0.18984661	0.186986143	0.184618427	0.182639526	0.180972732	0.179559957	0.178356271	0.177326306	0.176441808	0.175679918	
Blade spacing (in)	5.628686838	5.628686838	5.628686838	5.628686838	5.628686838	5.628686838	5.628686838	5.628686838	5.628686838	5.628686838	5.628686838	5.628686838	5.628686838	5.628686838	5.628686838	5.628686838	5.628686838	
Number of blades	24	27	29	30	31	32	33	34	34	35	35	35	35	36	36	36	36	
Blade solidity	1.421290655	1.421290655	1.421290655	1.421290655	1.421290655	1.421290655	1.421290655	1.421290655	1.421290655	1.421290655	1.421290655	1.421290655	1.421290655	1.421290655	1.421290655	1.421290655	1.421290655	
Power (hp)	36924.13015	45337.97373	49371.73549	53380.27295	55507.95492	57261.59554	58770.14915	60240.35176	61316.51644	61497.85783	62933.93278	62177.18197	62813.36025	62967.47132	63262.68709	63452.45417	63629.1731	
w_stage_ideal (BTU/lb)	6.656559251	7.012502276	7.387478473	7.782505594	8.198655813	8.637058633	9.09890396	9.585445321	10.09800328	10.637969	11.20680806	11.80606437	12.43736443	13.1024217	13.80304126	14.54112472	15.31867536	
w_stage_actual (BTU/lb)	22.69676029	27.86863543	30.34813389	32.81212731	34.11998446	35.19792348	36.12521086	37.0289244	37.69042818	37.80189626	38.68463199	38.21946756	38.61051769	38.70524767	38.88671279	39.00336003	39.11198675	
Stage Efficiency	0.863282352	0.821627041	0.813424472	0.807183817	0.810288967	0.81538546	0.821871304	0.828863726	0.837919569	0.851413634	0.859696644	0.878901854	0.892123742	0.908517966	0.924955209	0.942817232	0.961661908	
Pressure ratio	1.2	1.2	1.2	1.2	1.2	1.2	1.2	1.2	1.2	1.2	1.2	1.2	1.2	1.2	1.2	1.2	1.2	
Cumulative pressure ratio	1.2	1.44	1.728	2.0736	2.48832	2.985984	3.5831808	4.29981696	5.159780352	6.191736422	7.430083707	8.916100448	10.69932054	12.83918465	15.40702157	18.48842589	22.18611107	

Total power: 980844.8 hp